Journal of Human Evolution 127 (2019) 93–117

Contents lists available at ScienceDirect

Journal of Human Evolution

journal homepage: www.elsevier.com/locate/jhevol

New permanent teeth from Gran Dolina-TD6 (Sierra de Atapuerca). The bearing of *Homo antecessor* on the evolutionary scenario of Early and Middle Pleistocene Europe

María Martinón-Torres [a, b, *, 1], José María Bermúdez de Castro [a, b, *, 1], Marina Martínez de Pinillos [a], Mario Modesto-Mata [a, b], Song Xing [c, d], Laura Martín-Francés [e, a], Cecilia García-Campos [a], Xiujie Wu [c], Wu Liu [c]

[a] Centro Nacional de Investigación sobre la Evolución Humana (CENIEH), Paseo de la Sierra de Atapuerca 3, 09002, Burgos, Spain
[b] Anthropology Department, University College London, 14 Taviton Street, London WC1H 0BW, UK
[c] Key Laboratory of Vertebrate Evolution and Human Origins, Institute of Vertebrate Paleontology and Paleoanthropology, Chinese Academy of Sciences, Beijing, 100044, China
[d] CAS Center for Excellence in Life and Paleoenvironment, Beijing, 100044, China
[e] Univ. Bordeaux, CNRS, MCC, PACEA, UMR 5199 F_33615, Pessac Cedex, France

ARTICLE INFO

Article history:
Received 25 September 2018
Accepted 4 December 2018

Keywords:
Pleistocene
Human evolution
Europe
Sierra de Atapuerca
Gran Dolina
Teeth

ABSTRACT

Here we analyze the unpublished hominin dental remains recovered from the late Early Pleistocene Gran Dolina-TD6.2 level of the Sierra de Atapuerca (northern Spain), as well as provide a reassessment of the whole TD6.2 hominin dental sample. Comparative descriptions of the outer enamel surface (OES) and the enamel-dentine junction (EDJ) are provided. Overall, the data presented here support the taxonomic validity of *Homo antecessor*, since this species presents a unique mosaic of traits. *Homo antecessor* displays several primitive features for the genus *Homo* as well as some traits exclusively shared with Early and Middle Pleistocene Eurasian hominins. Some of these Eurasian traits were retained by the Middle Pleistocene hominins of Europe, and subsequently became the typical condition of the Neanderthal lineage. Although other skeletal parts present resemblances with *Homo sapiens*, TD6.2 teeth do not show any synapomorphy with modern humans. In addition, TD6.2 teeth can be well differentiated from those of Asian *Homo erectus*. The dental evidence is compatible with previous hypothesis about *H. antecessor* belonging to the basal population from which *H. sapiens*, *Homo neanderthalensis*, and Denisovans emerged. Future findings and additional research may help to elucidate the precise phylogenetic link among them.

1. Introduction

To date, the human fossil remains recovered from the TD6.2 level of the Gran Dolina cave site (Sierra de Atapuerca, Burgos, northern Spain) are the only ones available in the European hominin fossil record of the late Early Pleistocene, between the Jaramillo subchron and the Matuyama/Bruhnes reversal (Parés et al., 2018). This fact complicates the evaluation of the phylogenetic relationships of the fossils assigned by Bermúdez de Castro et al. (1997) to the species *Homo antecessor*, and the understandings of the origin and evolution of the European Early Pleistocene populations. New studies on several anatomical parts from the TD6.2 human hypodigm have revealed that some features, previously considered as Neanderthal autapomorphies, appeared during the Early Pleistocene (e.g., Gómez-Robles et al., 2007; Bermúdez de Castro et al., 2012). These traits, together with the expression of modern-like facial features in the TD6.2 hominins confer a special interest to the study of this human assemblage. The particular combination of skeletal and dental characteristics observed in the hominins of TD6.2 (Bermúdez de Castro et al., 2017a) suggests that *H. antecessor* is phylogenetically close to the divergence between Neandertals and modern humans. Pending the increase of the fossil record of the late Early and early Middle Pleistocene, the study of the TD6.2

* Corresponding authors.
E-mail addresses: maria.martinon@cenieh.es (M. Martinón-Torres), josemaria.bermudezdecastro@cenieh.es (J.M. Bermúdez de Castro).
[1] These authors have equally contributed to the elaboration of this article.

https://doi.org/10.1016/j.jhevol.2018.12.001
0047-2484/

sample appears crucial to explore the identity of the last common ancestor of *Homo neanderthalensis* and *Homo sapiens*. A more precise assessment of the relationships of *H. antecessor* with earlier and later hominin groups will undoubtedly shed light on the origin of the first Europeans and the pattern of hominin settlement of the European continent.

The last comprehensive study of the TD6.2 permanent teeth was published by Bermúdez de Castro et al. (1999a). Moreover, a short report about the TD6 deciduous teeth recovered during the first decade of the 21st century was published by Bermúdez de Castro et al. (2017b). Although some features of the teeth preserved in situ in the ATD6-96 and ATD6-113 mandibular specimens have been presented (Carbonell et al., 2005; Bermúdez de Castro et al., 2008), 14 unpublished teeth remain to be described. Some of these specimens have been virtually extracted by means of microcomputed tomography (μCT), a tool that we lacked in 1999. Here we present a comparative study of these new teeth. We expect that the presentation of this novel information, together with a reassessment of the entire TD6.2 sample of permanent teeth, will shed additional light on the understanding of the phylogenetic position of the TD6.2 hominins and their bearing in the evolutionary scenario of Early and Middle Pleistocene Europe.

1.1. The Gran Dolina TD6.2 level

The Gran Dolina cave site (TD) fills up a large cavity about 27 m deep and with a maximum width of 17 m. The stratigraphic section of the site was cut and exposed by the construction of a railway trench. Gil and Hoyos (1987) divided this section from bottom to top into 11 levels: TD1–TD11. However, the stratigraphy of the Gran Dolina site is under continuous refinement. The TD6 level has been divided into three sublevels (Bermúdez de Castro et al., 2012; Campaña et al., 2016): TD6.1, TD6.2, and TD6.3. The human fossils, as well as more than 300 artifacts and several thousands of micro- and macromammal fossil remains (Bermúdez de Castro et al., 1999b; Carbonell et al., 1999; Cuenca-Bescós et al., 1999; García and Arsuaga, 1999; van der Made, 1999) come from the sublevel TD6.2. Parés and Pérez-González (1995, 1999) observed a polarity reversal between TD7 and TD8, interpreted as the Matuyama/Brunhes boundary, meaning that levels TD8 to TD11 were deposited during the Middle Pleistocene, whereas levels TD7 to TD1 were deposited during the Early Pleistocene (see also a recent study by Álvarez-Posada et al., 2018). The combination of the paleomagnetic data and electron spin resonance (ESR)/U-series ages suggests an age range between 0.78 and 0.86 Ma for the TD6 level (Falguères et al., 1999). Thermoluminiscence (TL) dates on samples taken at the TD7 level, 1 m below the Brunhes/Matuyama boundary, give a weighted mean age of 0.96 ± 0.12 Ma for TD7 (Berger et al., 2008). The ESR dating applied to optically bleached quartz grains from TD6 gives dates between 0.60 ± 0.09 Ma and 0.95 ± 0.09 Ma (Moreno et al., 2015). These authors also obtained dates of 0.73 ± 0.13 Ma and 0.85 ± 0.14 Ma for the TD7 level, from samples taken under the Matuyama/Brunhes boundary. Using thermally transferred optically stimulated luminiscence (TT-OSL) dating of individual quartz grains, Arnold et al. (2015) obtained a weighted mean age of 0.84 ± 0.06 Ma for the TD6 level. Arnold and Demuro (2015) have undertaken a series of TT-OSL suitability assessments on known-age samples from TD6. Using this method, they obtained a weighted average age of 0.85 ± 0.04 Ma for TD6.3. The first direct ESR dating study of *H. antecessor* using one hominin tooth has provided a final age estimate ranging from 0.72 Ma to 0.95 Ma (Duval et al., 2018). Finally, a recent paleomagnetic study of the interior facies of TD1 place the TD6.2 hominins between the Matuyama/Brunhes boundary and the Jaramillo subchron (Parés et al., 2018). Summarizing, and taking into account the biostratigraphic information from TD6 (Cuenca-Bescós et al., 1999, 2015), we consider that the TD6 hominins could be assigned to the Marine Isotope Stage 21 (MIS 21).

2. Materials and methods

The present sample of permanent teeth from TD6.2 is curated at the Museo de Burgos, Spain. This sample comprises a total of 46 teeth (Table 1). The outer enamel surface (OES) morphology of 25 specimens was described by Bermúdez de Castro et al. (1999a), whereas the description of some features of the in situ teeth preserved in the mandibles ATD6-96 and ATD6-113 was carried out by Carbonell et al. (2005) and Bermúdez de Castro et al. (2008). Here we present the unpublished information of 14 specimens, including those unerupted in the immature maxillae ATD6-14 and ATD6-69 and in the immature mandibles ATD6-5 and ATD6-112, which were digitally extracted by means of μCT. The μCT images and related information are available upon request to the corresponding authors. Additional data of the in situ teeth of the adult mandibles ATD6-96 and ATD6-113 are also reported. Furthermore, we include a revision of the more diagnostic features of the specimens published and figured by Bermúdez de Castro et al. (1999a). Finally, and except for the trigonid crests pattern in the *H. antecessor* molars, we describe for the first time the enamel-dentine junction (EDJ) morphology of the TD6.2 permanent teeth. The evaluation of the morphological features has been made from the original fossils and the virtual images. The assignment of some of these teeth to a specific individual (from hominin H1 to hominin H8) can be found in Bermúdez de Castro et al. (2017c).

The mesiodistal (MD) and buccolingual (BL) dimensions of the TD6.2 were measured by J.M.B.C. to the nearest 0.1 mm, following the methods of Flechier, Lefèvre, and Verdéne (Lefèvre, 1973). For this purpose, we have used a specially designed calliper with wide, flat and thin tips, and moving arms that allows taking measurements in projection, when the reference points and planes are placed at different levels. The Lefèvre (1973) method is particularly useful when teeth are isolated but can be identically applied to both isolated and in situ teeth. MD diameter is easily affected by proximal wear, and is clearly decreased when occlusal wear is ≥ grade 5

Table 1
List of TD6.2 permanent teeth recovered so far. Previously unreported specimens are denoted by an asterisk. The TD6.2 teeth belong to a minimum of eight individuals (see Bermúdez de Castro et al., 2017b). The teeth of the mandible ATD6-5, the maxillary fragment ATD6-13, and the isolated teeth ATD6-1, 2, 3, 4, 6, 7, 8, 9, 10, 11, and 12 belong to the individual H1 (the holotype of *Homo antecessor*). The maxilla ATD6-69 belongs to individual H3. ATD-94 and ATD6-96 represent individual H5.

Specimens		
Tooth class	Right side	Left side
I^1		ATD6-14*
I^2	ATD6-143*; ATD6-69	ATD6-14*; ATD6-312
C^1	ATD6-69	ATD6-13; ATD6-14*
P^3	ATD6-7; ATD6-69	ATD6-13; ATD6-14*; ATD6-69
P^4	ATD6-8; ATD6-69	ATD6-9
M^1	ATD6-10; ATD6-69; ATD6-103*	ATD6-11; ATD6-69
M^2	ATD6-12	ATD6-69*
M^3		ATD6-69*
I_1		ATD6-52
I_2	ATD6-146*	ATD6-2; ATD6-48
C_1	ATD6-6	ATD6-1
P_3	ATD6-3	ATD6-96
P_4	ATD6-4; ATD6-125*	ATD6-96
M_1	ATD6-5; ATD6-94*; ATD6-112*	ATD6-96
M_2	ATD6-5; ATD6-144*	ATD6-96; ATD6-113

(Molnar, 1971). Fortunately, the TD6.2 teeth are generally unworn (grade 1 of the Molnar classification) or have little wear (grades 2 or 3). Apart from the MD and the BL, we have also calculated the computed crown area (MD × BL) and the measured crown area, following the technique described in Bermúdez de Castro et al. (1999a).

Besides the absolute dimensions we have obtained two indices (BL I^2/BL M^1) × 100 and (BL I_2/BL M_1) × 100. We selected the BL diameter as it is the least affected by occlusal wear, except in extreme cases where most of the crown is worn. We selected the lateral incisor because this tooth captures key changes when size expansion of the anterior teeth occurs, and the first molar because it is the most stable of the molar series. The TD6.2 measurements were compared with those of other hominins (Table 2 and Supplementary Online Material [SOM] Table S1). We have taken these measurements either from originals (Arago, Atapuerca-SH, Dmanisi, Montmaurin, Tighenif, Lazaret, La Quina 5, La Ferrasie 2, Hortus, Macassargues, and a recent human sample of aboriginals from Gran Canaria, Canary Islands) or from the literature (Blumenberg and Lloyd, 1983; Hershkovitz et al., 2018; and references listed in Bermúdez de Castro, 1986:Tables 5 and 6; Bermúdez de Castro et al., 1999a).

The descriptive terminology used in this report derives from the following sources: Carlsen (1987), Tobias (1991), Turner et al. (1991), Scott and Turner (1997), Martinón-Torres et al (2007, 2008, 2012:Table 4). The last reference includes a modified version of the Arizona State University Dental Anthropological System (ASUDAS) of scoring (Turner et al., 1991).

In order to study the morphological characteristics of the EDJ, the TD6.2 teeth were scanned using the Scanco Medical AG Micro-Computed Tomography 80 (70 kV and 114 μA) and the Phoenix v/tome/xs of GE Measurement & Control (100–120 kV, 110–140 μA and 0.2 Cu filter), housed at the Centro Nacional de Investigación sobre la Evolución Humana (CENIEH) in Burgos, Spain. The resultant slice thickness ranged between 18 and 36 μm for the former and between 27 and 36 μm for the latter μCT system. Tomographic data were processed and visualized with Amira 6.0.0. software (Visage Imaging, Inc., Berlin). The segmentation of the tissues was done semiautomatically with manual corrections and no filters were applied.

Comparison of the OES and EDJ surfaces were made with Pleistocene specimens from Africa and Eurasia obtained from different databases such as NESPOS (www.nespos.org) and ESRF paleontological microtomographic database (http://paleo.esrf.eu) and from the literature (Table 2). Aware of the lack of consensus in the taxonomic assignment of many specimens, we have used the terms *Homo erectus* sensu lato (s.l.), Asian *H. erectus*, or African *H. erectus*.

3. Results

3.1. Absolute and relative crown dimensions

In general, the mesiodistal (MD) and buccolingual (BL) crown dimensions of the TD6.2 teeth are large (Table 3) and comparable to those of the other African and Eurasian Early and Middle Pleistocene hominins (including Dmanisi), *H. erectus* s.l., and *Homo heidelbergensis* (Blumenberg and Lloyd, 1983; Bermúdez de Castro et al., 1999a; Zanolli et al., 2014). The smallest TD6.2 teeth are those belonging to ATD6-96, the M_3 being particularly reduced (Table 3). For the rest of the teeth, the dimensions exceed the mean values of the Atapuerca-SH hominins and the Neanderthals. It is important to point out that the anterior teeth of most Neanderthal specimens (e.g., Krapina) are characterized by having absolute and relatively large dimensions, comparable to those of the TD6 hominins. It is also interesting to note that compared to early *Homo* (*Homo habilis* and/or *Homo rudolfensis*), TD6 postcanine teeth have undergone a significant reduction whereas the anterior teeth have

Table 2
Pliocene and Pleistocene dental specimens included in the comparative sample.

Species/sample	Specimens
Paranthropus	SK 52; SK 55; SK 839; OH 5
A. afarensis	A.L. 128-23, A.L. 145-35, A.L. 161-40, A.L. 188-1, A.L. 198-1, A.L. 199-1, A.L. 200, A.L. 207-13, A.L. 241-14, A.L. 249- 26, A.L. 266-1, A.L. 277-1a, A.L. 288, A.L. 311, A.L. 315, A.L. 330, A.L. 333, A.L. 400, A.L. 417, A.L. 444, A.L. 486-1, A.L. 487, A.L. 620, A.L. 651; FEJEJ, LH-3, LH-4, LH-5, LH-6, LH-11, LH-14, LH-17; MAK-VP1/4, MAK- VP1/12
A. africanus	GVH-1; MLD2, MLD11, MLD18, MLD23, MLD28, MLD45; Sts12, Sts17, Sts22, Sts24, Sts52, Sts56, Stw13, Stw73, Stw151, Stw183, Stw252, Stw498; TM1514, TM1512 (see also Moggi-Cecchi et al., 2006)
H. habilis	KNM-ER 808, KNM-ER 1805, KNM-ER 1813; OH 6, OH 7, OH 13, OH 16, OH 21, OH 24, OH 39, OH 44; SK 27
Dmanisi[b]	D211, D2280, D2600, D2735, D2700, D4500
H. erectus s.s	Sangiran S4, S6, S7, S9, S17, S22, S1B, SB8103, BK7905, NG8503; Trinil[a]; Zhoukoudian PA66[a], PA67[a], PA68[a], PA110[a], PA69[a], PA70[a], PMU 25719, PMU M3550, PMU M3549, and PMU M3887 (Zanolli et al., 2018), and (Weidenreich, 1937), Yiyuan[a], Panxian Dadong[a], Xujiayao[a], Penghu 1 (Chang et al, 2014), Hexian[a], Konso-Gardula (Suwa et al., 2007)
East Africa late Early Pleistocene	Uadi Aalad (UA 222, UA 339) and Mulhuli-Amo (MA 93) (Buia) (Zanolli et al., 2014)
H. floresiensis	LB1, 2015 LB1, LB2/2, LB6/1, LB6/14, LB15/1, LB15/2 (Kaifu et al., 2015)
North Africa Middle Pleistocene	Tighenif I, II, and III[a], Rabat, Thomas Quarry, Casablanca, Jebel Irhoud (Hublin et al., 2017)
European Middle Pleistocene[c]	Atapuerca-SH[a], Arago[a], Mauer[a], Montmaurin[a], Pontnewyyd, Steinheim, Mala Balanica, BH-1 (Roksandic et al., 2011)
H. neanderthalensis	Anglin, Arcy II, Cabezo Gordo, Chateauneuf, Ehringsdorf, Engis II, Fondo Cattíe, Gibraltar (Devil's Tower), Kebara, Krapina, Kulna 1, La Ferrasie 2[a], La Quina 5[a], Lazaret I[a], Le Moustier 1, l'Hortus[a], Macassargues (isolated M2)[a], Malarnaud[a], Monte Circeo[a], Mosempron, Ochoz, Pech de l'Azé[a], Petit-Puymoyen, Pinilla del Valle (Madrid, Spain)[a], Saccopastore[a], Saint Cesaire, Shanidar, Sidrón (005,008), Tabun[a], Valdegoba[a], Vindija (G3), Zafarraya[a]
H. sapiens	Abri Pataud (1 and isolated teeth), Almonda (Zilhão, 1997), Brassempouy, Caldeirao (Trinkaus et al., 2001), Dolni Vestonicea, Mladec, Pavlov[a], Predmostí, Skhul (IV, V, VI), Misliya 1[a], Trou Magritte, Wad; Hispanic-Muslim medieval collection of San Nicolás (Murcia, Spain)[a], Canary Islanders[a]

Abbreviations: A.L. = localility from Hadar; FEJEJ = Fejej; LH = Laetoli; MAK-VP = Maka; GVH = Gladysvale; MLD = Makapansgat Limeworks Dumps; Sts = Sterkfontein; KNM-ER = Kenyan National Museum-East Rudolf; Sts = Sterkfontein; Stw = Swartkrans; TM = Transvaal Museum, Kromdraai; OH = Oldupai Gorge; SK = Swartkrans; LB = Liang Bua Cave.

[a] Observations made on original fossils. All other observations are from the cast collections of the American Museum of Natural History, New York USA, and the High Resolution Dental Casts Collection of the Universitat de Barcelona, Spain. When data were also collected from the literature, the reference is given.

[b] The Dmanisi hominins have been included in *Homo* aff. *ergaster* by Rosas and Bermúdez de Castro (1998), *Homo georgicus* by Gabounia et al. (2002), and *Homo erectus* by Rightmire et al. (2006, 2017). Due to its qualitative and quantitative importance, we prefer to use this sample as an independent identity.

[c] Considering that the Atapuerca-SH hominins have been excluded from *Homo heidelbergensis* (see Arsuaga et al., 2014), which represent the majority of the European Middle Pleistocene sample, and that there is no data from other African specimens included by some authors in this species, we prefer to avoid the use of this taxon.

Table 3
Measurements of mesiodistal (MD) and buccolingual (BL) diameters (in mm) of the TD6.2 permanent teeth. Non-erupted teeth or those in process of eruption could not be measured.

		MD	BL			MD	BL
I^1				I_1	ATD6-52	–	7.6
I^2	ATD6-69	8.3	8.2	I_2	ATD6-2	7.0	7.8
	ATD6-143	8.0	8.6		ATD6-48	7.8	7.7
					ATD6-146	7.4	7.0
C^1	ATD6-13	8.9	11.0	C_1	ATD6-1	8.1	10.0
P^3	ATD6-7	8.4	11.7	P_3	ATD6-3	8.8	10.6
	ATD6-69	8.8	11.5		ATD6-96	8.0	9.7
P^4	ATD6-8	8.1	11.6	P_4	ATD6-4	8.2	10.2
	ATD6-69	_	11.6		ATD6-96	7.6	9.4
					ATD6-125	8.3	10.5
M^1	ATD6-10	12.1	13.1	M_1	ATD6-5	12.2	11.8
	ATD6-69	11.9	12.1		ATD6-96	10.5	11.0
	ATD6-103	12.7	12.9		ATD6-94	13.0	11.8
M^2	ATD6-12	12.1	13.7	M_2	ATD6-5	13.5	12.0
					ATD6-96	12.3	11.0
					ATD6-113	13.0	11.6
					ATD6-144	13.8	11.6
M^3	–			M_3	ATD6-96	9.2	8.8
					ATD6-113	12.1	10.4

Table 4
Ratio between the buccolingual (BL) diameter of the upper lateral incisor (I^2) and the BL diameter of the upper first molar (M^1) (i.e., [BL I^2/BL M^1] × 100) in different hominins and hominin samples.

	BL I^2	BL M^1	(BL I^2/BL M^1) x 100
	(Range)		*n* X SD (Range)
AL 200-1a	7.3	13.3	54.9
LH-6	7.4	14.0	52.8
STS52	7.0	14.0	50.0
TM 1512	5.6	13.6	41.2
SK 55	6.3	14.4	43.7
SK 52	6.8	16.6	41.0
SK 839	6.0	14.0	39.3
OH5	7.6	17.7	42.9
KNM-ER 808	7.7	13.0	59.2
KNM-ER 1805	5.5	13.2	41.7
KNM-ER 1813	5.8	12.5	46.4
SK 27	7.6	13.2	60.1
OH 16	7.8	14.7	54.4
Dmanisi D2677/D2700	6.9	12.9	53.5
Sangiran 1B	10.0	13.7	73.0
Rabat	8.5	12.0	70.8
Thomas III	8.2	14.0	58.6
ZKD 01	8.0	12.4	64.5
KNM-WT 15.000	8.5	12.2	69.7
ATD6-69	8.2	12.1	67.8
Atapuerca-SH	(7.4–8.2)	(11.4–12.3)	5 66.4 1.8 (64.3–69.3)
Neanderthals	(7.7–9.2)	(11.3–13.1)	13 70.8 2.8 (66.6–76.4)
Skhul	(7.1–8.0)	(11.1–11.4)	4 64.5 6.1 (56.7–71.4)
Misliya 1	7.7	12.3	62.6
Qafzeh	(7.4–8.1)	(11.1–13.2)	5 62.8 4.2 (56.0–66.6)
Modern humans[a]	(5.6–7.3)	(10.0–12.0)	19 57.3 4.9 (47.8–65.2)

[a] Aboriginals (recent modern humans) from Gáldar, Gran Canaria (Canary Islands).

Table 5
Ratio between the buccolingual (BL) diameter of the lower lateral incisor (I_2) and the BL diameter of the lower first molar (M_1) (i.e., [BL I^2/BL M^1] × 100) in different hominins and hominin samples.

	BL I_2	BL M_1	(BL I_2/BL M_1) x 100
	(Range)		*n* X SD (Range)
AL 400-1A	7.5	12.7	59.0
A. africanus[a]	(6.5–8.5)	(11.3–13.0)	4 60.4 1.9 (57.6–61.8)
Paranthropus[b]	(6.4–8.1)	(13.5–15.4)	7 50.3 6.2 (41.8–51.9)
KNM-ER 820	6.2	10.7	57.9
OH 7	7.4	12.5	57.9
OH 16	7.6	12.8	59.4
Dmanisi D211	6.7	12.6	53.2
Dmanisi D2854/2735	7.4	11.2	66.1
KMN-WT 15000	8.2	11.2	73.9
Zhoukudian[c]	(6.7–7.3)	(10.6–10.9)	4 63.2 4.7 (58.4–68.9)
ATD6-2/ATD6-5[d]	7.8	11.8	66.1
Rabat	7.5	11.0	68.2
Mauer	7.8	11.2	69.6
Atapuerca-SH	(6.6–8.1)	(9.7–11.6)	14 69.9 2.9 (64.1–73.8)
Neanderthals	(7.0–8.7)	(9.8–12.1)	18 70.9 3.5 (63.8–78.1)
Skhul 4	7.1	11.2	63.4
Skhul 5	7.0	11.5	60.9
Modern humans[e]	(5.0–7.3)	(9.3–12.0)	97 57.8 4.1 (46.7–69.0)

[a] This sample includes the following specimens: MLD 18, STS 7, STS24, and STS 52.
[b] This sample includes *Paranthropus robustus* (SK 23, SK 34, SK 74, SK 845, and SK 858) and *Paranthropus boisei* (KNM-ER 3230 and Natron).
[c] This sample includes individuals A1, B1, G1, and H4 from Zhoukoudian.
[d] These teeth belong to the same individual.
[e] This sample is formed by aboriginals (recent modern humans) from the Canary Islands.

enlarged (Bermúdez de Castro et al., 1999a). Therefore, the absolute dimensions of the TD6 anterior and postcanine teeth are derived for the *Homo* clade. An additional and interesting question is whether the expansion of the anterior teeth in *H. antecessor*, a feature shared with all African and Eurasian Middle Pleistocene *Homo* specimens (Wolpoff, 1980), is quantitatively larger, smaller or similar to the degree of postcanine reduction.

In order to answer this question, we compared the BL diameter of the I^2 and M^1 of different hominins (Table 4). As expected, the index is particularly low in *Paranthropus*, since their anterior teeth are very small and their posterior teeth are extremely large (Fig. 1). The index is equally low in *Australopithecus*. In this genus, the posterior dentition is large, but the anterior teeth are clearly larger than in *Paranthropus* (Fig. 1). The primitive condition for the *Homo* clade is not very different from that observed in *Australopithecus*, whereas the value of the index tends to be larger in other Early and Middle Pleistocene *Homo*: *H. erectus* s.l., *H. antecessor,* and *H. neanderthalensis*. Note that the high index obtained in *H. neanderthalensis* is due to the high BL diameter of the I^2 (Fig. 1). The index is low in recent *H. sapiens*, due to a greater reduction of the postcanine teeth compared to the reduction in the anterior teeth (Table 4; Fig. 1). The index of early *H. sapiens* specimens such as Skhul, Qafzeh and Misliya 1 tend to have intermediate values between recent *H. sapiens* and Neanderthals. The index of the specimen ATD6-69 is close to that of *H. erectus* s.l., the Atapuerca-SH hominins, and some Neanderthals.

Similar results were obtained with the study of the lower dentition (Table 5). The index is low in *Paranthropus*, due to the great size of the postcanine teeth. Higher values of the index are obtained in *Australopithecus* and early *Homo* due to a significant reduction of the posterior teeth and no differences are found between them, although the small sample sizes call for caution.

Table 6
Main morphological enamel features of the TD6.2 permanent teeth according to ASUDAS modified version of Martinón-Torres et al (2012:Table 4).

Upper	Morphological enamel features
I^1	Shovel shape (grade 4) Labial convexity (grade 3)
I^2	Shovel shape (grades 4–5). Triangular shovel shape. Tuberculum dentale (grades 4–5) Labial convexity (grades 3–4)
C^1	Shovel shape (ASUDAS grade 4) Mesial marginal ridge (grade 1) Distal accessory ridge (grade 1) No developed cingulum.
P^3	Buccal essential ridge (grade 2) Lingual essential ridge (grade 2) Buccal cusp larger and taller than the lingual cusp. Position of the tip of the lingual cusp mesial compared to the tip of the buccal cup. Vestiges of buccal cingulum. Bulging of the upper half of the buccal face. $P^3 > P^4$
P^4	Buccal essential ridge (grade 2) Lingual essential ridge (grade 2) Buccal cusp larger and taller than the lingual cusp Tips of the lingual and buccal cusps aligned, except in ATD6-69 (like in P^3) Vestiges of buccal cingulum Bulging of the upper half of the buccal face $P_4 < P_3$
M^1	Skewed external outline with a bulging protrusion of the hypocone. Rhomboidal and compressed occlusal polygon. Largest cusp: protocone. Smallest cusp: metacone (grade 4) Carabelli (grade 2) No C5 (grade 0) Crista obliqua (grade 1) No transverse crest (grade 0) No mesial marginal accessory tubercles (grade 0) No parastyle (grade 0) Crenulated enamel surface (dendritic-like pattern) except ATD6-10 and ATD6-11 $M^1 < M^2$
M^2	Largest cusp: protocone Smallest cusp: metacone (grade 4) or hypocone (grade 3) Carabelli (grade 2 in ATD6-12, grade 0 in ATD6-69) C5 (grade 2 in ATD6-12, grade 0 in ATD6-69) Crista obliqua (grade 1) No transverse crest (grade 0) No mesial marginal accessory tubercles (grade 0) No parastyle (grade 0) Crenulated enamel surface (dendritic-like pattern) $M^2 > M^1$
M^3	Reduced No other morphological description is possible
Lower	**Morphological enamel features**
I_1	Shovel shape is faint (grade 1) Labial convexity is pronounced (grade 4) Tuberculum dentale (grade 0) Buccolingually expanded
I_2	Shovel shape (grade 2–3) Labial convexity (grade 3–4) Tuberculum dentale (grade 0) Buccolingually expanded
C_1	Shovel shape (ASUDAS grade 3) Lingual marginal ridges are well developed (especially the distal one)
P_3	Transverse crest (grade 2) Lingual cusps (grade 5) Strongly asymmetrical outline Remarkable talonid Large occlusal polygon Marginal ridges that connect with the cingulum Two roots (mesiobucal root with two pulp canals and distolingual root with a single canal) $P_3 > P_4$
P_4	Transverse crest (grade 1–2) Lingual cusps (grade 5) Asymmetrical outline Mesially displaced metaconid Remarkable talonid Large occlusal polygon Two roots (mesiobucal root with two pulp canals and distolingual root with a single canal) $P_4 < P_3$
M_1	Anterior fovea (grade 2) Discontinuous mid-trigonid crest (grade 1) except ATD6-112 (grade 2) Discontinuous distal trigonid crest (grade 1) No deflecting wrinkle (grade 0) except ATD6-5 and ATD6-94 (grade 2) C5 (grade 4–5) No C6 (grade 0) except ATD6-94 (grade 2) No C7 (grade 0) except ATD6-94 (grade 2) No protostylid (grade 0) Y-pattern Crenulated enamel surface (dendritic-like pattern) $M_1 < M_2$
M_2	Anterior fovea (grade 2) Discontinuous mid-trigonid crest (grade 1) except ATD6-5 and ATD6-94 (grade 2) Discontinuous distal trigonid crest (grade 1) No deflecting wrinkle (grade 0) C5 (grade 4–5) No C6 (grade 0) No C7 (grade 0) except ATD6-5 (grade 3) No protostylid (grade 0) Y-pattern Crenulated enamel surface (dendritic-like pattern) Mesotaurodontism and hypotaurodontism
M_3	Anterior fovea (grade 0) except ATD6-113 (grade 2) Discontinuous mid-trigonid crest (grade 1) except ATD6-113 (grade 2) Discontinuous distal trigonid crest (grade 1) No deflecting wrinkle (grade 0) C5 (grade 3–4) C6 (grade 1–2) No C7 (grade 0) except ATD6-5 (grade 4) No protostylid (grade 0) except ATD6-96 (grade 1) Y-pattern (except ATD6-96) Crenulated enamel surface (dendritic-like pattern) Mesotaurodontism and hypertaurodontism Reduced

Homo erectus s.l. and *H. antecessor* exhibit a greater value of the index, due to an even greater reduction of the postcanine teeth. In contrast, the Atapuerca-SH hominins and the Neanderthals share a relative increase of the anterior dentition with regard to the postcanine dentition, yielding a high BL I_2/BL M_1 index. As in the upper dentition, this index suggests that the TD6 hominins are placed in an intermediate situation between early *Homo* and the Atapuerca-SH/Neanderthals specimens, showing a balanced size relationship between the anterior and posterior dentition (see additional analyses concerning this feature in Bermúdez de Castro, 1999a).

The size relationship between M_1 and M_2 can be evaluated in the mandibles ATD6-5 (H1) and ATD6-96 (H6). In both cases M_1 is smaller than M_2. Using the computed crown area (MD × BL), in ATD6-96 the values are M_1 (115.5) < M_2 (135.5). In ATD6-5 the values are M_1 (143.9) < M_2 (162.0). The size relationship between the M_1 and M_2 in TD6.2 is primitive for the genus *Homo*, a condition which is also present in *Australopithecus* and *Paranthropus* (Wolpoff, 1971). The $M_1 < M_2$ size relationship is almost a constant in *H. erectus* s.l., and *H. heidelbergensis* (Mauer, Arago 13, and Arago 2), with the exception of OH 22, Thomas 1, Arago 89, and interestingly in the specimens D 211 and D 2735 from Dmanisi (but not in D 2600). Some of the Middle Pleistocene hominins show a

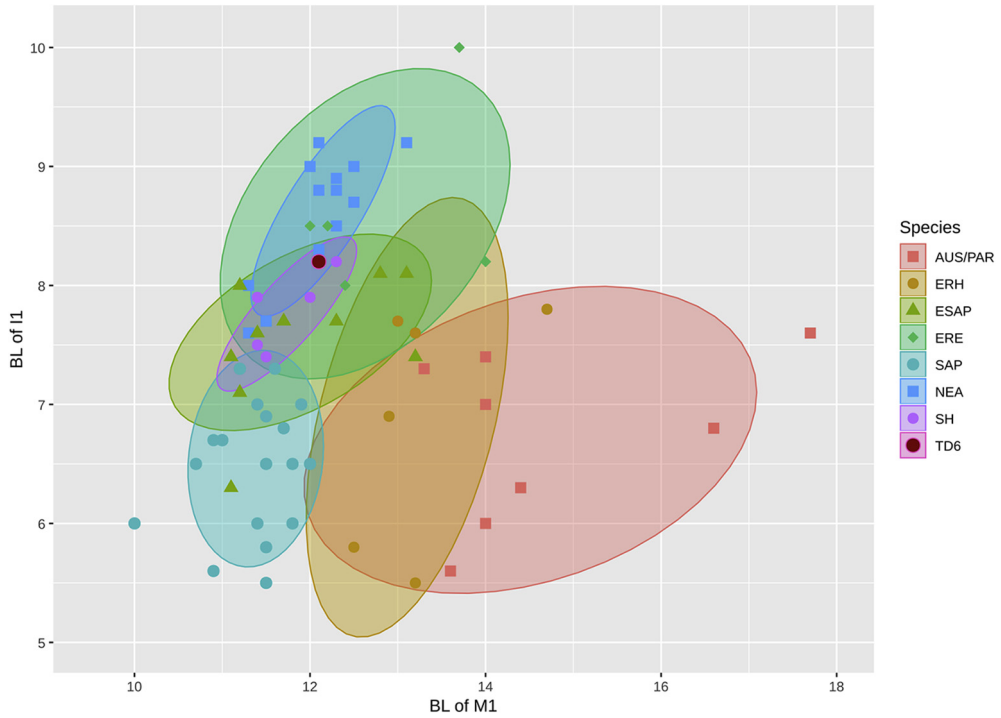

Figure 1. Scatterplot representing the buccolingual diameter (BL) of the M1 (x axis) and the BL of the I2 (y axis). Ellipses of equiprobability ($p = 0.8$) are represented for each species. AUS/PAR = *Australopithecus/Paranthropus*; ERH = early *Homo*; ESAP = early *Homo sapiens*; ERE = *Homo erectus*; SAP = *Homo sapiens*; NEA = *Homo neanderthalensis*; SH = Sima de los Huesos; TD6 = *Homo antecessor*.

similar size relationship between M_1 and M_2, such as KNM-BK 8518 and Tighenif 2. However, the derived condition, $M_1 > M_2$, appeared in Eurasia during the Middle Pleistocene, and can be found in specimens such as ZKD G1, ZKD K1, and ZKD 17 from Zhoukoudian, Montmaurin (France) and most of the Atapuerca-SH individuals.

Concerning the maxillary dentition, and using the computed crown area, the pattern in individual H1 is M^1 (158.5) < M^2 (165.8). This is the primitive pattern for the *Homo* clade, and is also the usual pattern in *Australopithecus* and *Paranthropus* (Wolpoff, 1971). Except in D 2282, Sangiran 17, ZKD H3, and Petralona, the $M^1 < M^2$ pattern is the norm in the Early and Middle Pleistocene hominins. The condition, $M^1 > M^2$ appeared in Europe during the Middle Pleistocene, according to our observations, in the Atapuerca-SH hominins. This derived condition is also frequent in Neanderthals and modern humans.

Additional information on the crown index and other interdental indices of the TD6.2 dental sample can be found in Bermúdez de Castro et al. (1999a).

3.2. OES and EDJ morphology

Upper central incisors (I^1): ATD6-14 This tooth has been virtually extracted from the maxilla by means of μCT, so it is the first time that the morphology of an upper central incisor from *H. antecessor* can be studied (Fig. 2). It belongs to an immature individual so approximately one-third of the crown and the whole root are not yet developed. The crown presents a longitudinal linear fracture along its mesial marginal ridge. From the buccal and the lingual aspects, the contour is rectangular, and the marginal ridges run parallel. There are several longitudinal wrinkles running along the enamel labial surface. From the lingual aspect, we identify a pronounced shovel shape (grade 4) where the distal marginal ridge is slightly shorter than the mesial one (Table 6). From half of the preserved crown, two strong ridges or spines are present, corresponding to a tuberculum dentale of grade 4. Unfortunately, labial convexity cannot be fully assessed since approximately the cervical third is missing, but there is at least a moderate labial convexity (grade 3).

At the dentine level, both marginal ridges are parallel and particularly marked, forming a pronounced shovel shape (Fig. 3). While the enamel wrinkles at the labial and lingual surface are clearly visible, at the dentine we can see only traces of two ridges that would correspond to the tuberculum dentale. Although the incompleteness of the crown prevents a proper assessment of the labial convexity, ATD6-14 presents at least weak to moderate convexity.

The degree of labial convexity in early *Homo* and African Early Pleistocene hominins tends to be weak and never exceeds a grade 3 (e.g., OH-16, KNM-ER 1590) whereas the expression of this feature in the Early Pleistocene specimens from Asia ranges from moderate to strong (e.g., S7-48). With a grade 3, ATD6-14 would be in between the Early Pleistocene African and the East Asian groups, and would be similar to that of the I^1 D2736 from Dmanisi. Shovel shape is a variable feature in both its degree and frequency of expression (e.g., Irish, 1993; Crummett, 1995), but the highest degree of shoveling (grades 5 and 6) is characteristically found in the Neanderthal lineage, although isolated exceptions can be also identified in the Middle (e.g., ZKD 2 and ZKD PA-66 from Zhoukoudian) and Late Pleistocene (Tongzi) fossils from Asia. The pronounced shovel shape of ATD6-14 exceeds the degrees usually found in the Early Pleistocene fossils from Africa and Asia, including D2736 from Dmanisi, and is closer to that found in the Middle Pleistocene hominins from Europe, Asia and the Neanderthals. Regarding the morphology of the lingual surface, ATD6-14 shows two finger-like extensions that can be considered as primitive and similar to the spines developed by other Early Pleistocene hominins from Africa (e.g., KNM-ER 1590; KNM-WT 15000) and Early and Middle Pleistocene hominins from Asia (ZKD 2, Yuanmou, Panxian Dadong).

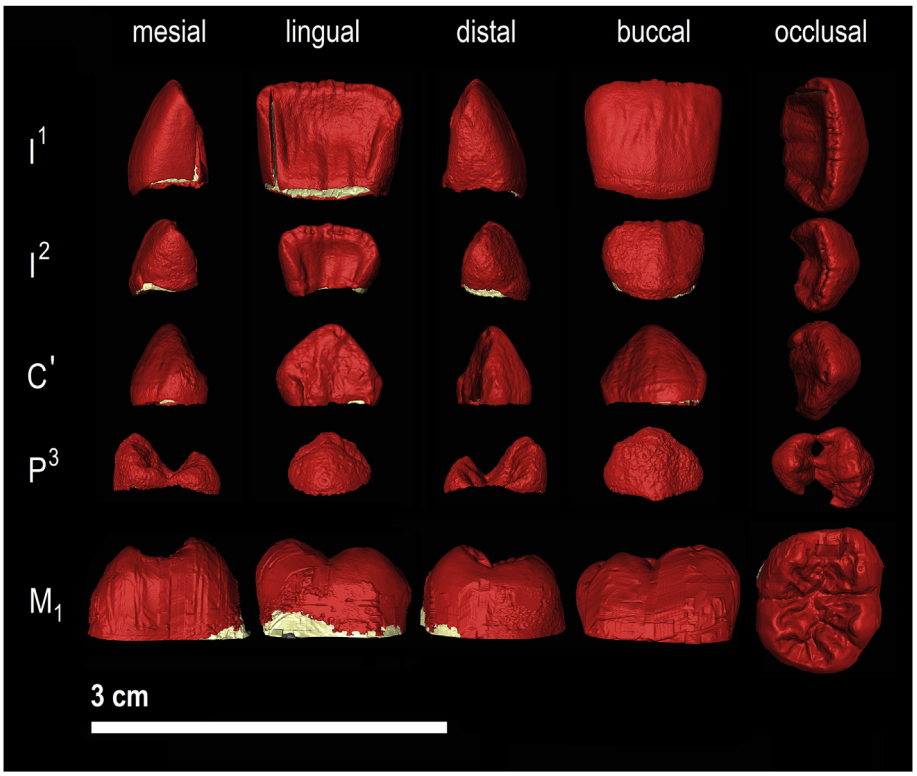

Figure 2. Virtual images of the crown of the permanent teeth included in the maxilla ATD6-14 and in the mandible ATD6-112 (immature individuals H2 and H8, respectively). The maxilla of the H2 includes from the left I^1 to the left P^3, whereas the mandible ATD6-112 includes the M_1.

Although the crown is not complete, it seems that a well-circumscribed basal eminence, as is typically found in European Middle Pleistocene hominins, Neanderthals, and some East (S7-1, S7-48) and West Asian Early Pleistocene specimens (D2736), is absent in ATD6-14.

The smooth labial surface of ATD6-14 at the EDJ contrasts with the remarkable expression of labial wrinkles at the EDJ and the pulp cavity limits of Asian specimens such as Zhoukoudian (PA66) and Hexian (PA835) I^1 (Xing et al., 2014, 2018).

Upper lateral incisors (I^2): ATD6-312, ATD6-143, ATD6-69, ATD6-14 The state of preservation is excellent except for a small crack at the root tip of ATD6-143 (Fig. 4). ATD6-312 is a dental germ and the cervical third of the crown and the roots are not developed. ATD6-14 is still inside the immature maxilla ATD6-14 (Bermúdez de Castro et al., 1999a) and has been virtually extracted by means of μCT (Fig. 2).

From both the labial and lingual aspects, the crowns display a subrectangular contour, where the mesial marginal ridge is larger than the distal one, so the incisal edge ascends distally. Compared to ATD6-312 and ATD6-14, the marginal ridges of ATD6-143 are less parallel and diverge towards the incisal edge, in a similar way to ATD6-69 I^2. The marginal ridges are greatly thickened (grade 5 of shovel shape) and the tuberculum dentale is pronounced (grade 4 in ATD6-312 and grade 5 in ATD6-143; Table 6). In ATD6-14 the marginal ridges are also thick, showing shovel shape of grade 4. In ATD6-312, the tuberculum dentale is attached to the distal marginal ridge, as also happens in ATD6-69, whereas in ATD6-143, there is a groove separating the two. In ATD6-143 and ATD6-312 we identify a deep and narrow longitudinal groove in the lingual surface. In ATD6-143 (as in ATD6-69) this groove divides the inflated essential ridge into two components. In addition, in these teeth, the mesial marginal ridge is separated from the essential ridge by an additional groove. In ATD6-14 there is a pronounced narrow depression that divides the essential ridge into two components. From the occlusal aspect, ATD6-143, and ATD6-14 show pronounced labial convexity (grade 4) whereas in ATD6-312 the convexity is moderate (grade 3). In all the specimens, the deep longitudinal groove and angled incisal edge contribute to the 'V' occlusal section characteristic of the 'triangular shovel shape' (Martinón-Torres et al., 2007, 2012). The root of ATD6-143 is robust and relatively straight. From the lateral view, the labial side is more convex than the lingual one. There is a moderate longitudinal depression running along its distal surface that constricts the oval-shaped section of the root. The root apex of ATD6-69 remains open (stage G of the Demirjian et al., 1973 classification).

The marginal ridges are also thickened at the dentine level forming a pronounced shovel shape. The distal marginal ridges are shorter than the mesial ones and both tend to diverge towards the incisal edge (Fig. 3). This feature, together with the deep longitudinal groove in the lingual surface, provides the distinctive triangular shovel shape at the EDJ also. Except for the incomplete crown of ATD6-14, the other three specimens exhibit a pronounced tuberculum dentale at the EDJ. The strongest tubercle is from that of ATD6-143, and it is separated from the distal marginal ridge by a groove. The free apex is connected to a well-developed longitudinal ridge that runs towards the incisal edge. This finger-like ridge is placed between the distal marginal ridge and the deep longitudinal groove that, in ATD6-143 and ATD6-312, divides the essential ridge into two components. The labial convexity of the specimens is ranged between the weak degree in ATD6-312 to very strong in ATD6-14, ATD6-69 and ATD6-143.

Labial convexity in *H. antecessor* I^2 ranges from moderate to strong. With a few early *H. sapiens* exceptions (DV15, and Qafzeh 6 and 15), the highest degree of expression for this feature is exclusive to the Early (e.g., S7-2, S7-56) and Middle Pleistocene (ZKD 6,

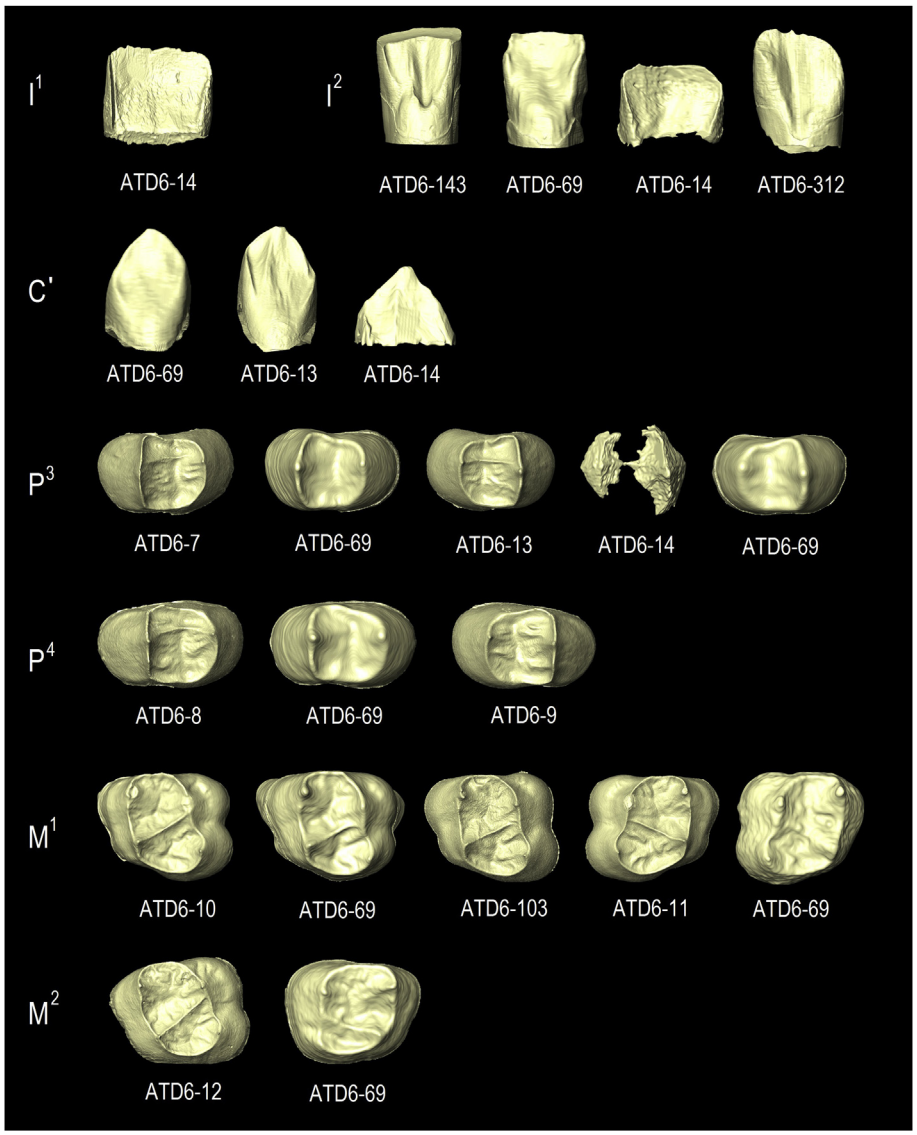

Figure 3. The EDJ surfaces of the upper permanent TD6.2 teeth obtained from μCT. The images are not scaled.

ZKD 7, Atapuerca-SH) populations from Eurasia and Neanderthals. A labial convexity weaker than degree 3 is observed in UA 22 from Buia (Zanolli et al., 2014). Shovel shape is also marked in the TD6.2 hominins. However, the particularity of *H. antecessor* relies not on the degree of expression of the marginal ridges (which is at the upper limit of the Early Pleistocene populations from both Asia and Africa) but in the expression of a type of triangular shovel shape (Martinón-Torres et al., 2007, 2012). TD6 hominins present an incipient form of this triangular shovel shape, where the marginal ridges diverge towards the incisal edge instead of running parallel, and the lingual fossa is slightly more spacious than in European Middle Pleistocene populations and Neanderthals. A similar marginal ridge development was noticed by Mizoguchi (1985) in the Sangiran and Zhoukoudian assemblages. The expression of a pronounced tuberculum dentale (≥3) is also infrequent in other Early Pleistocene populations from Africa with the isolated exception of KNM-ER 808 and OH-39. *Homo antecessor* I^2 are also different from that found in the Early Pleistocene locality from Buia, Eritrea (Zanolli et al., 2014), which lacks shovel shape and a distinct tuberculum dentale. Overall, this "mass-additive" (term by Irish, 1993) combination of features found in *H. antecessor* I^2 is absent in the African Early and Middle Pleistocene populations from Africa (with possibly one exception, that of the Middle Pleistocene specimen OH-29) and falls in the so-called Eurasian dental pattern (Martinón-Torres et al., 2007).

Upper canines (C^1): ATD6-13, ATD6-14, ATD6-69 The C^1 ATD6-14 has been virtually extracted from the maxilla ATD6-14. This tooth belongs to an immature individual so less than half of the crown and the whole root are not yet developed (Fig. 2). The description of the crown of the canine included in the maxilla ATD6-69 was carried out by Bermúdez de Castro et al. (1999a), but this is the first time that this tooth has been virtually extracted from this specimen and can be observed in its whole.

The C^1 of ATD6-14 is perfectly preserved. In both lingual and buccal views, this tooth exhibits a pentagonal contour with the distal occlusal arm being longer and more inclined than the mesial one. The mesial marginal ridge is larger than the distolingual one, but it is not possible to know if it was attached to a tuberculum dentale (grade 1 of mesial canine ridge; Table 6). A marked ridge is present at the lingual face, near the mesial marginal ridge, but since the crown is not completed it is not possible to ascertain the morphology of the tuberculum dentale. The C^1 of ATD6-69 is also

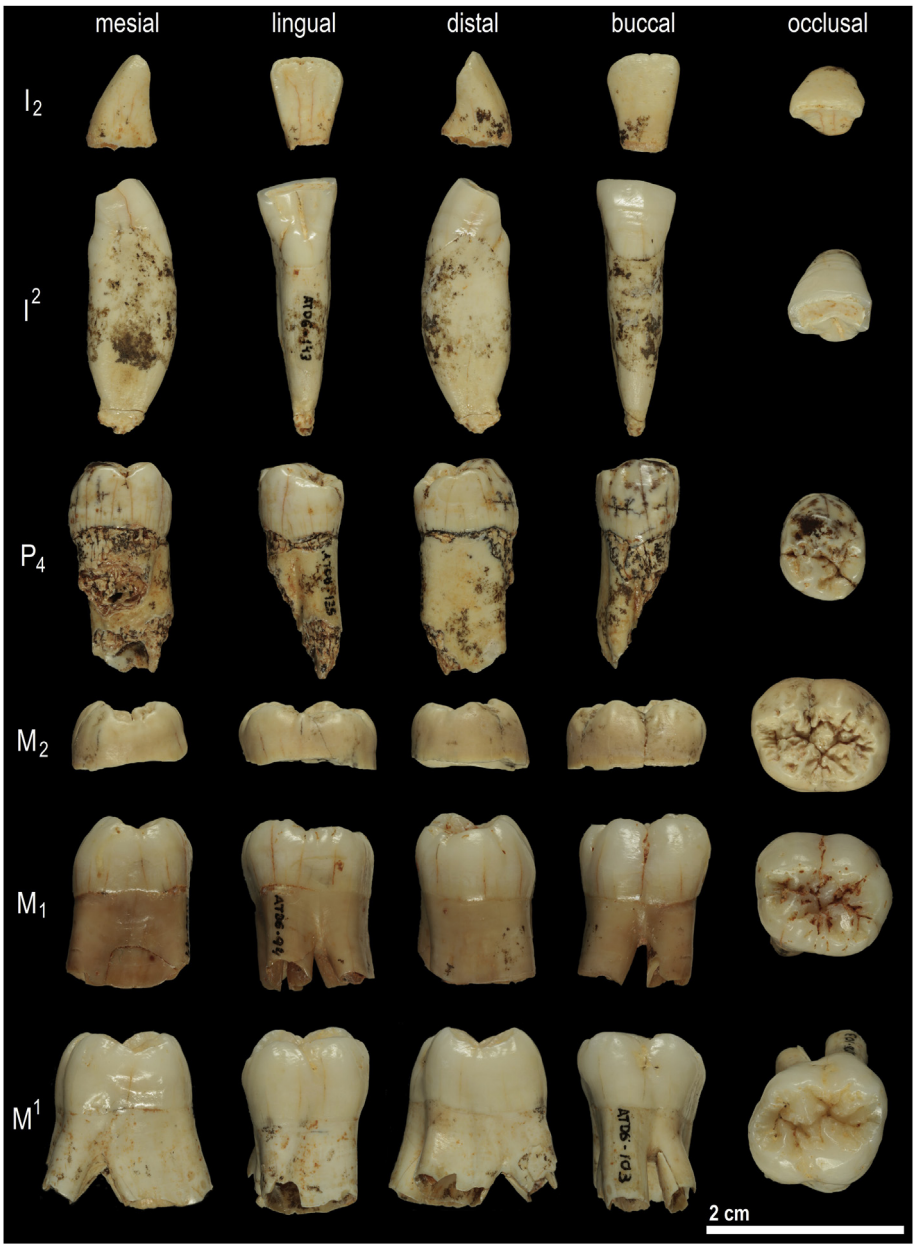

Figure 4. Some of the TD6.2 permanent teeth: I_2 ATD6-146; I^2 ATD6-143; P_4 ATD6-125; M_2 ATD6-144; M_1 ATD6-94; and M^1 ATD6-103. Bermúdez de Castro et al. (1999a,b) and Bermúdez de Castro et al. (2008) published images of the TD6.2 permanent teeth recovered during the 1990s, as well as those of particular specimens recovered during the first years of the 21st century.

well preserved. This tooth did not reach the occlusal plane, so it is unworn (grade 1). As in the C^1 of ATD6-14 and ATD6-13, the occlusal edge of ATD6-69 is asymmetrical, the mesial cutting edge being shorter and less inclined than the distal one. The marginal ridges are clearly pronounced forming a shovel shape of grade 4. The mesial marginal ridge in both canines is somewhat larger than the distal one (grade 1 of mesial canine ridge). The upper half of the buccal face shows some grooves and gentle enamel wrinkles running vertically along the crown. In both C^1 the lingual face exhibits a strong essential ridge, separated by a groove from the mesial marginal ridge and delimited by the central grove. The distal accessory ridge is barely expressed in both ATD6-13 and ATD6-14 (grade 1). The roots are single, long and mesiodistally compressed. The developmental state of the ATD6-69 root matches stage F of Demirjian et al. (1973).

Regarding the inner morphology of the upper canines (Fig. 3), we can see the asymmetry between the shorter mesial cutting edge and the large distal one. The marginal ridges, particularly the mesial ones, are pronounced, and in both ATD6-13 and ATD6-14, the essential ridge adopts the shape of a conspicuous ridge that runs from the basal eminence towards the incisal edge. Due to the incompleteness of the crown, we cannot assess the presence of a tuberculum dentale in ATD6-14, but there are traces of ridging in ATD6-13 and ATD6-69.

The well-preserved C^1 from Dmanisi, D 2732 is one of the best references to explore the primitive morphology of this tooth class in early *Homo*. The canine of Dmanisi has a symmetrical contour viewed buccally or lingually, with both mesial and distal edges showing the same length. The marginal ridges are thickened and tubercle-like, well delimited in both the lingual and labial surfaces.

Moreover, the Dmanisi canine exhibits a prominent essential ridge, and a strong basal cingulum is expressed along the labial surface (Martinón-Torres et al., 2008). These features are similar to those described in *Australopithecus africanus* and *H. habilis* (Robinson, 1956; Tobias, 1991). This primitive morphology undergoes a deep change in other later *Homo* populations; while the cingulum and/or a sharply pointed cusp are present in some *H. erectus* s.l. (e.g., KNM-WT 15000), the tubercle-like marginal ridges are lost. Although these tubercle-like ridges are present in the deciduous canine of the ATD6-14 specimen (Bermúdez de Castro et al., 1999a), permanent TD6.2 canines have lost these features. Overall, the C^1 of TD6 show a derived morphology with regard to early *Homo*, and despite the crown and root robustness, the morphology is incisor-like. Compared to later *Homo,* such as Neanderthals and *H. sapiens,* the thick marginal ridges and the inflated essential ridge confer a less derived aspect to the TD6.2 canines. The root of the TD6.1 C^1 is mesiodistally compressed, so it departs from the conical shape seen in the Dmanisi and Asian *H. erectus*.

Upper third premolars (P^3): ATD6-7, ATD6-13, ATD6-14, left and right ATD6-69 The only unpublished TD6.2 P^3 was virtually extracted from the maxilla ATD6-14. Only a minimal part of the crown was developed, which includes the lingual and buccal cusps. They are joined by the mesial marginal ridge and by the buccal and lingual essential ridges (Fig. 2), which are apparently connected by a transverse crest (grade 1). The buccal cusp is taller than the lingual one.

In all the P^3 the buccal cusp is clearly larger and taller than the lingual cusp (Table 6). On average, the area of the buccal cusp of the P^3 of the H1 (ATD6-7 and ATD6 13) and H3 (right and left P^3 of ATD6-69) represents 59.7% of the total measured crown area (Bermúdez de Castro et al., 1999a). Although we cannot obtain the computed crown area of the cusps of the P^3 of ATD6-13, it is evident from Figure 2 that the buccal cusp is also greater than the lingual cusp. The tip of the lingual cusp is mesially displaced with regard to the tip of the buccal cusp. The buccal essential ridge is bifurcated (grade 2) in the P^3 of the H1 and H3. The lingual essential crest is also bifurcated (grade 2), but the ridges are less conspicuous (except in the right P^3 of ATD6-69, see Bermúdez de Castro et al., 1999a). All the P^3 display a distal accessory ridge. The sagittal fissure is slightly convex in all TD6 P^3. It separates the main cusps and ends in deep, fissure-like and buccally-placed anterior and posterior foveae. The sagittal fissure cuts both the mesial and the distal marginal ridges and delimits minor accessory tubercles. In occlusal view, the upper half of the buccal surface is remarkably bulging, although a well-developed cingulum is missing. In mesial and distal views, the buccal bulging is also evident. The upper region of the buccal face is furrowed by some enamel ridges delimited by shallow occlusal-cervical grooves that could represent the vestige of a cingulum. The massive roots of the P^3 of individual H1 bifurcate 5 mm away from the cervical enamel junction into a buccal and a lingual component. Each radical has its own canal and they are joined by a dentine/cementum sheet. The developmental state of the ATD6-69 root matches stage F of the Demirjian et al. (1973) classification.

At the dentine level, the lingual cusp is smaller than the buccal one, and the tip is slightly mesially displaced with regard to the tip of the buccal one (Fig. 3). The occlusal surface is complicated by the expression of several ridges. In the buccal cusp, ATD6-7 shows three dentine ridges that could potentially correspond to a bifurcated essential crest and a distal accessory ridge, whereas the ridges at the lingual cusp could correspond to a bifurcated lingual cusp. The ridges are similar in ATD6-13, although less pronounced than in ATD6-7. The occlusal surface of ATD6-69 is remarkably simpler, but we have to be cautious with this statement since the resolution of the scan of the in situ teeth is lower than that of the isolated specimens. It is interesting to note a thin but continuous transverse crest connecting the main cusps in both ATD6-7 and ATD6-13, absent from ATD6-69 premolars. These continuous crests are not reflected at the OES. Due to the early state of crown development in ATD6-14, we can only assess that the buccal cusp is taller than the lingual one, and looking at the enamel we could predict a continuous transverse crest at the dentine.

Apparently, the morphology of permanent upper premolars is not taxonomically very discriminative (Martinón-Torres et al., 2008). However, the geometric morphometric study of the occlusal outline of the P^3 carried out by Gómez-Robles et al. (2011a) found some discriminant features which allow one to distinguish a primitive morphology from a derived one. The significant reduction of the lingual cusp and the generally symmetric crown outline of the TD6 P^3 can be considered derived features for the genus *Homo* that are present in the Atapuerca-SH hominins and the Neanderthals. However, the TD6 P^3 do not show the reduction of the occlusal polygon characterizing the Neanderthals and the Atapuerca-SH hominins (Gómez-Robles et al., 2011a). Interestingly, the Arago P^3 (Arago 7, Arago 16, and Arago 36) are more primitive than the TD6 P^3 by having buccal and lingual cusps of similar area and by the obliquity of their sagittal fissure.

The contour of Zhoukoudian PA67 P^3 is more asymmetrical than that of TD6 P^3 (Xing et al., 2018). Furthermore, and unlike the P^3 of TD6.2, PA67 exhibits a continuous transverse crest, a feature which is more frequent in Asian *H. erectus* (ZKD 16, Sangiran 4, Sangiran 7–35, Xichuan PA543, and Hexian PA832). It is also present in Dmanisi D3672 and a few Atapuerca-SH specimens, and very rare in African *H. erectus* (Xing et al., 2018). The presence of this feature in the LB1 P^3 and its almost total absence in the P^3s of *H. sapiens* lead Kaifu et al. (2015) to consider the expression of a transverse crest the primitive condition for the *Homo* clade. However, beyond characteristically higher frequencies in Asian *H. erectus*, the taxonomic utility of these features may be limited.

Another interesting aspect is the bulging buccal surface of the TD6 P^3, a feature shared with the European and Middle Pleistocene hominins and the Neanderthals, as well as with Asian *H. erectus* (Lumley et al., 1972; Bermúdez de Castro, 1988; Martinón-Torres, 2006; Xing et al., 2018). This feature is not present in *H. habilis*, African *H. erectus* (Kimbel et al., 1997) and Dmanisi P^3 (Martinón-Torres et al., 2008). It seems, therefore, that the bulging of the buccal face could be a derived trait of the Eurasian Early and Middle Pleistocene *Homo* species. The bulging is not present in *H. sapiens*, but its absence may be related to the general reduction of the dentition in this species.

Also noteworthy is the robustness of the roots, similar to that of other Pleistocene hominins included in *H. erectus* s.l., like Zhoukoudian (PA67) or the Arago specimens. Despite that, the root morphology is simpler than the three-rooted specimens found within *Australopithecus*, *H. habilis* (KNM-ER, 1808), Hexian (PA832), and some specimens from the East Asian Early Pleistocene of Pucangan (Sangiran 7–35; Ward et al., 1982; Wood, 1991, Grine and Franzen, 1994; Moggi-Cecchi et al., 2006; Xing et al., 2018).

TD6.2 P^3 have a remarkably relatively simple and smooth EDJ surface, a feature shared with most hominins from the genus *Australopithecus*, *Paranthropus* and *Homo* (Xing et al., 2018). In contrast, the EDJ surface of the Yiyuan P^3 (Sh.y.003 and Sh.y.004) is complicated with a dendrite-like pattern characterized by interconnected ridges, and bifurcated essential crests (Xing et al., 2016). This pattern is characteristic of the premolars and molars of some East Asian Middle Pleistocene hominins classified as 'classic' *H. erectus* (see Xing et al., 2018).

In summary, and despite their large size, robustness and complicated occlusal morphology (e.g., bifurcated essential crest) common to other Early and Middle Pleistocene specimens, the TD6

P^3 are generally derived with regard to the *Homo* clade. In particular, the TD6 P^3 are more derived than the P^3 of Asian *H. erectus*, and interestingly, than the P^3 of the Middle Pleistocene site of Arago.

Upper fourth premolars (P^4): ATD6-8, ATD6-9, ATD6-69 As in the P^3, the buccal cusp of the TD6.2 P^4 is larger and taller than the lingual cusp. On average, the area of the buccal cusp of the P^4 of the H1 (ATD6-8 and ATD6 9) and H3 (right P^4 of ATD6-69) represents 57.8% of the total measured crown area (Bermúdez de Castro et al., 1999a). This percentage is similar to that obtained for the TD6.2 P^3. The cusp apices of both main cusps are centered and aligned in ATD6-8 and ATD6-9, whereas the tip of the lingual cusp is mesially displaced with regard to the tip of the buccal cusp in ATD-69. The essential crests are bifurcated in the lingual cusps of ATD6-8 and ATD6-9, and in the buccal cusp of ATD6-69 (grade 2). All premolars show mesial and distal accessory ridges, particularly pronounced in ATD6-6 and ATD6-9. The sagittal fissure is continuous and gently convex, except in ATD6-8 that displays a mesial and very thin but continuous transverse crest. As in the P^3 the sagittal fissure bifurcates at the mesial and distal ends, delimitating minor accessory tubercles. Particularly, in the right P^4 of ATD6-69 there is a mesiobuccal and two distobuccal accessory tubercles. In occlusal view, the upper half of the buccal surface is remarkably bulging, a feature that is also noticeable from the mesial and distal views. No buccal cingulum is present in these teeth, although, like in the P^3, the lower half of the buccal face is furrowed by shallow wrinkles and grooves. The lingual surface is more vertical than the buccal one. The massive root system comprises a buccal and a lingual radical which bifurcate about 5.0–7.0 mm below the cement-enamel junction and are joined by a dentine/cementum sheet. The developmental state of ATD6-69 root matches stage F of the Demirjian et al. (1973) classification.

Concerning the EDJ, and as happens in the P^3, the lingual cusps of all the P^4 are smaller than the buccal ones and the tips are mesially displaced but more centered with regard to each other (Fig. 3). ATD6-8 exhibits a continuous transverse crest connecting the tips of both main cusps. The buccal and lingual cusps of both ATD6-8 and ATD6-9 are bifurcated and show well-marked distal and mesial accessory ridges. In both cases, the strong distal accessory ridge marks a tip or small shoulder along the buccal aspect of the occlusal rim. ATD6-8 presents a continuous transverse, whereas it is absent in its antimere. Once again, the lower scan resolution of ATD6-69 complicates the description of the dentine morphology. Although the crest is clearly bifurcated at the OES this is less obvious at the EDJ. Similarly, the accessory ridges are less clear and it seems that a continuous transverse crest is absent. Despite their presence at the OES, the accessory marginal tubercles are less evident at the EDJ.

In general, the aspect of the TD6.2 P^4 is robust and primitive. However, like in the P^3 some features are derived with regard to the genus *Homo*. The relative size of the lingual cusp in ATD6.2 P^4 is different from the one usually found in *Australopithecus* and early *Homo* (Sperber, 1973; Tobias, 1991). However, this feature is variable and while the lingual cusp is larger than the buccal cusp in D2282 from Dmanisi, the opposite occurs in D2700 (Martinón-Torres et al., 2008). A lingual cusp of similar size or somewhat greater than the buccal one is observed in PA68 from Zhoukoudian (Xing et al., 2018) and other *H. erectus* s.l. specimens, like those of Sangiran, Yiyuan, KNM-ER 15000, and KNM-ER 3733 (Xing et al., 2018). In *H. sapiens* there is a tendency to have a relatively wider buccal cusp.

The geometric morphometric analysis carried out by Gómez-Robles et al. (2011a) separated those P^4 with an asymmetric crown, a large lingual cusp relative to the buccal cusp, a mesially placed lingual cusp and a broad occlusal polygon from others. Interestingly, Arago 26, the P^4 of Steinheim, and the P^4 of some Neanderthals (e.g., Renne 8), share these features and the same morphospace with earlier hominins (e.g., *Paranthropus* and some *H. habilis*). In contrast, the TD6.2 specimens are revealed as more symmetrical, with a reduced lingual cusp relative to the buccal cusp, and a shortened axis between both foveae (Gómez-Robles et al., 2011a). Most Asian *H. erectus*, the Atapuerca-SH hominins and most Neanderthals plot within the same region as the TD6.2 P^4, thus suggesting that all of them share the Eurasian pattern defined by Martinón-Torres et al. (2007).

The buccal and lingual cusps of the TD6.2 P^4 are separated by a continuous sagittal groove. This feature is observed in some *H. erectus* s.l., like ZKD 25 and ZKD 133', Sangiran 4, Sangiran 7–3, KNM-ER 1803, Arago 26, most Atapuerca-SH specimens and Neanderthals, as well as in *H. sapiens*. In contrast, the presence of a continuous or interrupted transverse crest between the buccal and lingual cusps is observed in some in other *H. erectus* s.l., such as D2282, PA68, ZKD 27, Sangiran 7–29, and KNM-ER 3733, *Australopithecus* and early *Homo*. Kaifu et al. (2015) considered that the presence of a transverse crest is the primitive condition for the *Homo* clade, due to the practical absence of this feature in *H. sapiens*. However, and as in the P^3, it seems that this feature is a polymorphic trait in fossil *Homo* and, therefore, of restricted utility despite its higher frequency in Eurasian early and Middle Pleistocene specimens.

In some early hominins, like the D2282, ZKD 28, Sangiran 7–3, and KNM-ER 1803, the buccal surface is vertical (Kimbel et al., 1997), whereas in later Pleistocene hominins this surface bulges (e.g., Sangiran 4, or PA 68). Again, the polymorphic status of this feature prevents us from assessing its taxonomical utility (Martinón-Torres et al., 2008). Importantly, TD6.2 P^4 have lost the buccal cingulum usually present in early hominins, although the expression of some buccal wrinkles and grooves could represent a vestige of it.

The presence of two or three independent roots (coalesced or not) is the norm in *Australopithecus*, early *Homo* and *H. erectus* s.l (Wood, 1991; Moggi-Cecchi et al., 2006; Martinón-Torres et al., 2008). In the P^4 of TD6.2 the two roots are separated but joined by a dentine/cementum sheet, and form a robust structure, particularly in ATD6-9 (Bermúdez de Castro et al., 1999a).

The relatively simple and smooth EDJ surface of the TD6.2 P^4 contrasts with the dendrite-like EDJ surface of the Yiyuan P^4 (Sh.y.007 and Sh.y.071; Xing et al., 2016).

Like the P^3, the P^4 from TD6.2 show an overall primitive aspect, but a detailed analysis reveals that some features are derived with regard to the *Homo* clade. Although the TD6.2 P^4 share a Eurasian pattern with Asian *H. erectus*, and the P^4 of Arago, they are more derived in features such as the relative reduction of the lingual cusp.

Upper first molars (M^1): ATD6-10, ATD6-11, left and right ATD6-69, ATD6-103 Bermúdez de Castro et al. (1999a) described specimens of ATD6-10, ATD6-11 and ATD6-69. However, ATD6-103 was unpublished (Fig. 4). This tooth exhibits minimal enamel attrition (grade 2) indicating a very short duration of functional occlusion before death. The mesiolingual part of the root, which is the best preserved one, measures 9.2 mm (Bermúdez de Castro et al., 2010), and it is at stage F of the Demirjian et al. (1973) classification. ATD6-103 exhibits some enamel crenulations with a similar degree of complexity as those of the almost unworn M^1 of ATD6-69. ATD6-103 exhibits a rounded rhomboidal occlusal contour, with a protruding hypocone (Hy; Table 6). The protocone (Pr) is the largest cusp, followed by the hypocone, the paracone (Pa), and the metacone (Me; Gómez-Robles et al., 2011b). This size relationship is similar to that of the M^1 from the H1, the holotype of *H. antecessor* (ATD6-10 and ATD6-11), but different

from that of ATD6-69 (Pr > Pa > Hy > Me). The C5 is absent in the sample, with the possible exception of ATD6-69, and there is neither marginal accessory tubercle (grade 0) nor parastyle (grade 0). A Carabelli pit is present in ATD6-103 (grade 2), and the crista obliqua is continuous (grade 1), although it shows a shallow depression at the level of the central fissure, as in ATD6-69. In ATD6-10 and ATD6-11, the crista obliqua is also continuous. A deep fissure-like posterior fovea runs parallel to the distal marginal ridge and is bounded by the essential crest of the hypocone and a distal ridge of the metacone. The transverse crest joining the protocone and the paracone is interrupted by the prolongation of the central fissure, as in ATD6-10 and ATD6-69. This crest is absent in ATD6-11.

ATD6-103 exhibits a similar occlusal outline as the other TD6.2 M^1, as was described by Gómez-Robles et al. (2007) in their geometric morphometric study. This outline is characterized by a rhomboidal occlusal polygon, a relative distal displacement of the lingual cusps and protrusion in the external outline of a large and bulging hypocone.

The roots of ATD6-10 and ATD6-11 bifurcate at about 4.0–4.5 mm from the cervical line and are clearly divergent (see a detailed description in Bermúdez de Castro et al., 1999a). The root apex of the M^1 of ATD6-69 is closed. In this tooth the bifurcation is a little higher, but the roots are not divergent.

Regarding the dentine morphology of the M^1, none of them exhibits a C5 (Fig. 3). The metacone and hypocone are large in the case of ATD6-69, and very large in ATD6-10, ATD6-11 and ATD6-103. The bulging and protruding hypocone gives the molar a rhomboidal occlusal contour. While the transverse crest is absent, the oblique crest is continuous in all the specimens. Whereas there is no expression of parastyle, the Carabelli's complex is present in all individuals, being a small relief without a free apex in ATD6-10 and ATD6-11, a large Y-shape depression in ATD6-103 (grade 3 from Ortiz et al., 2012) and a pit in ATD6-69 (grade 2 from Ortiz et al., 2012). Moreover, small mesial marginal accessory tubercles are also present in all M^1 except for ATD6-69, but the lower scan resolution could affect the identification.

Following the geometric morphometric analysis carried out by Gómez-Robles et al. (2007), the shape of the TD6.2 M^1 is derived with regard to the hominin clade. The same derived morphology is present in the Atapuerca-SH hominins and the Neanderthals, whereas the primitive morphology (*Australopithecus* and early *Homo*) is characterized by an approximately squared occlusal polygon and a regular contour in which no cusp protrudes in the external outline (Gómez-Robles et al., 2007; Martinón-Torres et al., 2013). *Homo erectus* s.l. and *H. sapiens* retain the primitive shape and, thus, they exhibit a squared contour. Furthermore, the distance between the lingual cusps in these species does not exceed the distance between the buccal cusps, and the occlusal polygon is expanded in relation to the external contour (Gómez-Robles et al., 2007). The same configuration is present in the Arago specimens (Arago 21, Arago 31, and Arago 54).

Unlike the TD6.2 M^1, *Australopithecus,* early *Homo*, as well as Dmanisi and *H. erectus* from Sangiran tend to express a well-developed transverse crest connecting the mesial aspects of the protocone and the paracone. The expression of a continuous crista obliqua seems to be frequent from the Middle Pleistocene onwards, but its variable frequency in earlier hominins prevents the drawing of taxonomic conclusions (Martinón-Torres, 2006).

The TD6.2 M^1 exhibit the hominin general pattern of a relatively simple a smooth EDJ surface. This pattern contrasts with the complicated and dendrite-like pattern observed in the Hexian PA836 specimen (Xing et al., 2014).

Upper second molars (M^2): ATD6-12, ATD6-69 The right M^2 from ATD6-69 has been virtually extracted from the maxilla (Fig. 5). This tooth is at stage E of development in the Demirjian et al. (1973) classification. The root of this tooth grew to the level of the bifurcation of the lingual and buccal radicals, and measures about 5.0 mm. Like ATD6-12 (Bermúdez de Castro et al., 1999a), the occlusal surface is largely complicated by the presence of enamel crenulations. In ATD6-12 the protocone is the largest cusp, followed by the paracone, hypocone (grade 5), and metacone (grade 4; Table 6). In the M^2 of ATD6-69 the size order of the cusps is Pr > Pa > Me > Hy. In this tooth, the metacone is large (grade 4), whereas the hypocone is reduced (grade 3). In ATD6-12, the hypocone protrudes in the distal aspect of the occlusal contour in a similar pattern as in the M^1, but not in ATD6-69. In both ATD6-12 and ATD-69 the crista obliqua is continuous (grade 1), although there is a shallow depression at its midpoint, at the level of the central fissure. A Carabelli pit is present in ATD6-12 (grade 2), as well as a small C5 (grade 3). In our reconstruction of the M^2 of ATD6-69 it seems that there is no expression of the Carabelli complex. The C5 is also absent in this tooth (grade 0), but there is a small tubercle placed at the mesiobuccal corner. The transverse crest is absent (grade 0) in both ATD6-12 and ATD6-69. In ATD6-12, the radicals are remarkably divergent from the crown base and among them (see Bermúdez de Castro et al., 1999a:Fig. 4).

The inner morphology of ATD6-12 is characterized by a complex pattern where, in addition to the main cusps, there are

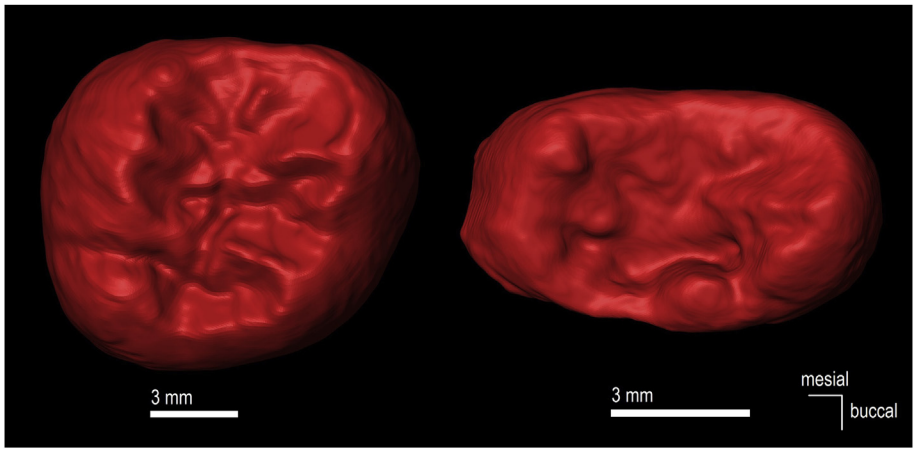

Figure 5. This picture shows virtual images of the crowns of the left M^2 (left in the image) and the left M^3 (right in the image) included in the maxilla ATD6-69 (Hominin 3, H3). The lower scan resolution of these specimens makes it difficult to give a thorough description of the dentine morphology of the M^3.

several ridges. However, the EDJ of ATD6-12 does not reach the complexity of the dendrite-like pattern of *H. erectus* s.s. (Xing et al., 2018:Figs 2 and 5). While the hypocone of ATD6-69 is medium-sized, in ATD6-12 the hypocone is large and protruding. None of the specimens presents a C5 at the EDJ, although ATD6-12 shows a small but clear one at the OES. There is no sign of a parastyle and only a pit-like Carabelli's trait in the case of ATD6-12 is present.

The occlusal contour of ATD6-12 resembles that of *Australopithecus*, early *Homo* and *H. erectus* s.l. because of the skewed distobuccal aspect of the crown, and the strong development of the hypocone (Tobias, 1991; Martinón-Torres, 2006; Moggi-Cecchi et al., 2006). The M^2 of ATD6-69 also shows a skewed distobuccal outline of the crown, with reduction of the metacone. However, this tooth shows a stronger hypocone reduction than ATD6-12. A considerable reduction of the hypocone is characteristic of the Atapuerca-SH hominins and some Neanderthals, so the occlusal contour adopts a subtriangular and heart shape (Bermúdez de Castro, 1988; Bailey, 2002; Martinón-Torres, 2006). However, among the European Middle Pleistocene hominins, we highlight the M^2 of Arago because of its rectangular primitive aspect, with well-developed metacone and hypocone.

The presence of a C5 or even multiple distal tubercles placed in a buccal position is characteristic of *Australopithecus* (Robinson, 1956; Moggi-Cecchi et al., 2006), *H. habilis* (Tobias, 1991), Dmanisi (Martinón-Torres et al., 2007), and Arago 21. In ATD6-12 there is a small C5, but this cusp is absent in the M^2 of ATD6-69.

The absence of crista obliqua seems to be a primitive feature, as observed in the majority of *Australopithecus*, early *Homo*, and *H. erectus* s.l., including Dmanisi (Wood and Engleman, 1988; Martinón-Torres, 2006; Martinón-Torres et al., 2007) and, interestingly, in Arago 14 and Arago 21. The frequent expression of a continuous crista obliqua in later hominins, like the Atapuerca-SH, Neanderthals and *H. sapiens*, would support this conclusion (Bermúdez de Castro, 1988; Bailey, 2002; Martinón-Torres, 2006).

As in the M_1 the general relatively simple and smooth EDJ surface of the TD6.2 M^2 differs from the dendrite-like pattern observed in the EDJ surface of the M^2s P833 and PA837 from Hexian (Xing et al., 2014).

Upper thirds molars (M^3): ATD6-69 This tooth has been extracted virtually from the maxilla ATD6-69 and its development is not finished (stage B of development of Demirjian et al., 1973). The cuspal enamel was not totally formed and the morphology of the crown was not complete. Due to the lack of contrast between the enamel and the dentine it is not possible to reconstruct the EDJ. The only morphological information we can recover from this tooth is the strong reduction of the distal cusps (Fig. 5).

With regard to this, it is interesting to mention that, with some isolated exceptions (e.g., Denisova and Xujiayao), the majority of hominin specimens show a remarkable reduction of the M^3 distal cusps compared to the M^1 and M^2 (Martinón-Torres et al., 2008 and references therein).

Lower central incisors (I_1): ATD6-52 The description of this tooth was carried out by Bermúdez de Castro et al. (1999a). It is interesting to highlight that shovel shape in ATD6-52 is faint (grade 1) but the labial convexity is pronounced (grade 4; Table 6). Furthermore, the marginal ridges are not divergent and no tuberculum dentale is observed (grade 0). The long root is mesiodistally compressed with wide and shallow mesial and distal longitudinal grooves. It measures about 17.6 mm. This length was taken on projection, from the enamel-dentine junction at the buccal face to the apex (see Bermúdez de Castro, 1988).

Although the lower central incisor ATD6-52 is broken (Fig. 6), at the EDJ, the preserved distal marginal ridge hints at a faint shovel shape. The convexity of the labial surface is pronounced and the cingular region of the lingual surface is smooth, which means that no tuberculum dentale is expressed.

Within the hominin fossil record, the permanent first lower incisors show low intra- and inter-population variability, at least regarding the expression of shovel shape. Nevertheless, it is interesting to mention ATD6-52 does not show divergent marginal ridges, a primitive feature observed in Dmanisi, *H. habilis* (OH 7, OH 16), *Homo ergaster* (KNM-WT 15.000, KNM-ER 820), and *H. erectus* (Sangiran 7, ZKD 5, 56, 58), the Rabat specimen (Martinón-Torres et al., 2008), as well as in UA 369 from Buia (Zanolli et al., 2014).

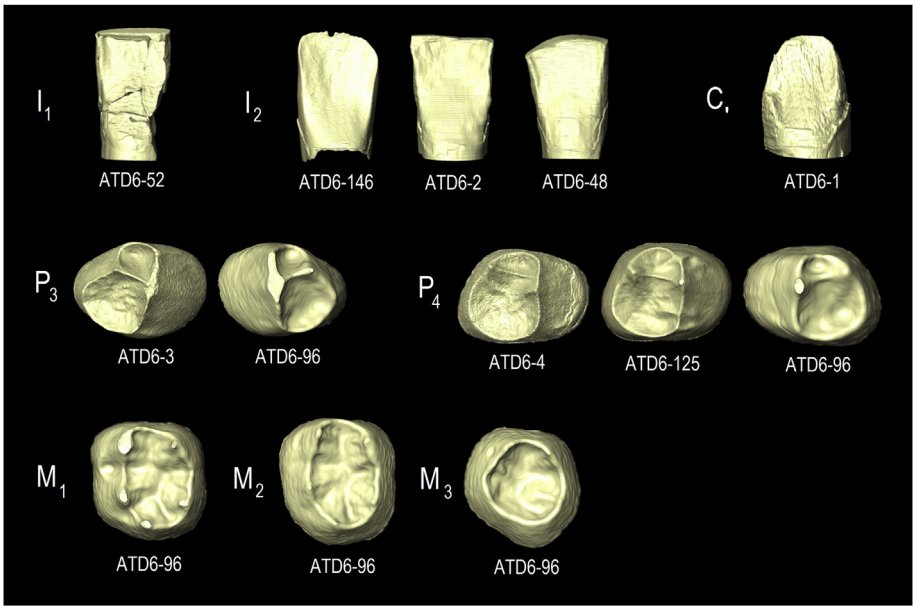

Figure 6. The EDJ surfaces of the lower permanent TD6.2 teeth obtained from μCT. The EDJ of the molars of the mandibles ATD6-5, ATD6-112, ATD6-113, as well as that the isolated specimens ATD6-94 and ATD6-144 are figured in Martínez de Pinillos et al. (2017). The images are not scaled.

In contrast, the marginal ridges are more parallel, as in Mauer, the Atapuerca-SH hominins, and *H. neanderthalensis*. The labial convexity of ATD6-52 is greater than that of D 211, and outside the range of variation of the African Plio-Pleistocene specimens (Martinón-Torres et al., 2008).

Lower lateral incisors (I_2) ATD6-2, ATD6-48, ATD6-146 Bermúdez de Castro et al. (1999a) described the specimens ATD6-2 and ATD6-48, but ATD6-146 was unpublished (Fig. 4). ATD6-146 wear is in grade 1 and the crown is almost complete. In this tooth, the mesial and distal marginal ridges diverge from the neck to the incisal edge, like ATD6-48 (see Bermúdez de Castro et al., 1999a:Fig. 5). In ATD6-2, the mesial ridge is almost vertical and only the distal one diverges. The three I_2 show faint marginal ridges producing a shovel shape varying from grade 2 (ATD6-48) to grade 3 (ATD6-2 and ATD6-146). The buccal convexity is pronounced (grade 4) in ATD6-2 and ATD6-146, and moderate (grade 3) in ATD6-48 (Table 6). Although the three specimens exhibit a clear basal eminence, the lingual surface is smooth (grade 0 of tuberculum dentale).

Regarding the dentine of the I_2, all of them present a clear basal eminence without traces of ridging or tubercles (Fig. 6). The labial surface of ATD6-2 and ATD6-48 exhibit a pronounced convexity, while in ATD6-146 it is moderate. In contrast with the degrees of expression at the OES, ATD6-2 and ATD6-48 show traces of shovel shape, whereas in ATD6-146 this feature is faint. At the enamel, the three specimens present a clear divergence of the edges, however at the dentine this aspect is less evident. The marginal edges are almost vertical and parallel one to another, and only the distal edge of ATD6-48 diverges towards the incisal surface.

Perhaps the more striking difference between the TD6 I_2 and those of the African specimens assigned to *Australopithecus*, *H. habilis* and African *H. erectus* is the pronounced convexity of the labial surface. In the African specimens, this surface tends to be flat or barely convex (Tobias, 1991), a feature also observed in modern humans (Martinón-Torres et al., 2012) and in the I_2 from D211. In contrast, the specimen D3698 from Dmanisi exhibits a moderate curvature (Martinón-Torres et al., 2007), similar to that observed in the TD6.2 I_2. The same degree of labial convexity (grades 2–3) is observed in Asian *H. erectus* (e.g., Sangiran S-18, Sangiran 7–50, ZKD10, ZKD 12), Rabat, Arago, Mauer, the Atapuerca SH specimens, and Neanderthals (Martinón-Torres et al., 2012). Thus, this feature seems to be characteristic of the Eurasian dental pattern (Martinón-Torres et al., 2007).

Shovel shape in I_2 within the genus *Homo* is generally faint, similar to that of the TD6.2 specimens, and is not particularly helpful for taxonomic debates (Weidenreich, 1937; Tobias, 1991; Moggi-Cecchi et al., 2006; Martinón-Torres et al., 2007). The divergence of the mesial and distal ridges seems to be more marked in African Pleistocene *Homo*, like OH7 and KNM-WT 15000, whereas in TD6.2 and other populations, such as Asian *H. erectus*, European Middle Pleistocene hominins and Neanderthals, the marginal ridges run parallel to each other. Nevertheless, the divergence is also remarkable in ATD6-48 (Bermúdez de Castro et al., 1999a:Fig. 5), so this tooth, in particular, would have preserved a more primitive conformation. Like I_1, the morphology of I_2 has limited taxonomic value, and the lingual surface rarely express pronounced shovel shape or tuberculum dentale.

Lower canines (C_1) ATD6-1, ATD6-6 ATD6-1 was described by Bermúdez de Castro et al. (1999a), and presents a grade 3 shovel shape with a well-developed essential ridge (Table 6). ATD6-6 is only a fragment of crown of the right C_1 from individual H1, the holotype of *H. antecessor*. At the dentine level, this specimen exhibits a pronounced distal marginal ridge that merges with the basal eminence (Fig. 6). This marginal ridge is also marked at the buccal surface by a vertical groove. The mesial marginal ridge is also elevated but less pronounced than the distal one. In lingual view, the essential ridge is pronounced and well delimited. Although ATD6-6 is broken and only the distal part is preserved, the distal marginal ridge seems less pronounced than its antimere, ATD6-1.

The morphology of the TD6.2 lower canines can be considered incisor-like and remarkably different from the primitive pattern exhibited by *Australopithecus*, early *Homo* specimens and the Dmanisi hominins. The primitive conformation in the genus *Homo*, like the one exhibited by D211 and D2735 from Dmanisi, consists of a markedly asymmetric crown in occlusal view, so the tip of the canine is mesial to the buccolingual mid-plane of the crown. Furthermore, apart from well-developed mesial and distal marginal ridges that adopt the shape of an independent tubercle in the case of the distal one, primitive canines display a prominent essential ridge that occupies the totality of the lingual surface. Additionally, these teeth show a remarkable labial cingulum (Martinón-Torres et al., 2008). This primitive morphology changes around the Early to the Middle Pleistocene transition, so that *H. erectus* s.l. shows a more incisor-like morphology (Weidenreich, 1937; Brown and Walker, 1993; Grine and Franzen, 1994). Nevertheless, it is important to note the presence of a buccal cingulum in the various C_1 from Zhoukoudian (Weidenreich, 1937), in that from Yiyuan (Xing et al., 2016), and in those from the North African Middle Pleistocene (Rabat, Tighenif, and Sidi-Abderrahaman), which is however absent in TD6.2. Furthermore, from the figures of Weidenreich (1937) a residual distal cuspule can be identified in some of the Zhoukoudian specimens (ZKD 70, ZKD 71, and ZKD 73).

Summarizing, the crown of ATD6-1 shows a derived morphology for the genus *Homo*. Except for the size and robustness of this tooth, the morphology of ATD6-1 is very similar to that of the European Middle Pleistocene hominins (Mauer, Arago, Atapuerca-SH, Lazaret, and the Neanderthals), with a variable expression of the marginal ridges and a shovel shape that range from slight to pronounced (grades 1 to 4; Martinón-Torres et al., 2012). In ATD6-1, the shovel shape may be grade 3. The essential ridge can be easily seen in ATD6-1, as in Mauer, Arago 24, and Arago 101, but not in SH hominins or Mountmaurin and Neanderthals. However, even in these cases, the essential ridge never reaches the degree of development of *Australopithecus*, early African *Homo*, Dmanisi, *Homo floresiensis* and some of the Zhoukoudian C_1 (Weidenreich, 1937;

Figure 7. Occlusal view of the premolars of the mandible ATD6-96.

Robinson, 1956; Johanson et al., 1978; Tobias, 1991; Martinón-Torres et al., 2008; Kaifu et al., 2015).

Lower third premolars (P_3): ATD6-3, ATD6-96 A detailed description of ATD6-3 was carried out by Bermúdez de Castro et al. (1999a), and some notes about the P_3 of ATD6-96 were published in Carbonell et al. (2005). The P_3 of this mandible is well preserved (Fig. 7) and shows a grade 3 of occlusal wear. The buccal cusp is flattened and exhibits a clear diamond-shape dentine patch. The primitive aspect of ATD6-3 and ATD6-96 is remarkable. Although ATD6-3 is larger than ATD6-96, their morphology is very similar. In both cases, the occlusal contour is asymmetrical, with a marked projection of the distolingual part of the crown, and a more bulging mesial part of the buccal surface (Table 6). The buccolingual axis of the tooth is clearly oblique in relation to the mesiodistal axis. The tip of the lingual cusp is mesially displaced and connected with the buccal cusp by a transverse crest (grade 2). The lingual cusp is narrow and distal to it there is a conspicuous talonid where up to four accessory cusps (grade 5) are developed, with one of them at the distobuccal aspect of the talonid. The anterior fovea is delimited by the transverse crest and the mesial marginal ridge. It is particularly deep in ATD6-3. The geometric morphometric analysis carried out by Gómez-Robles et al. (2008) showed that both ATD6-3 and ATD6-96 share the same morphospace in the relative warp analysis as the majority of early hominins, due to the asymmetrical morphology and the expanded talonid. While the cingulum is vestigial in ATD6-96, it is well pronounced in the case of ATD6-3, where two deep mesiobuccal and distobuccal grooves form a clear U-shape.

Of particular interest is the root complex of this tooth. Although a preliminary assessment of ATD6-96 P_3 based on an X-ray concluded that this tooth was single-rooted (Carbonell et al., 2005), the analysis of this mandible with a μCT reveals that the same complex morphology as described in ATD6-3 is present: a distolingual (DL) component with a root canal and a plate-like mesiobuccal (MB) component with two independent root canals (2R: MB + DL). In ATD6-96, the root bifurcates about 5.0 mm from the cervical line, followed by the bifurcation of the canals. This process leads to the formation of a DL radicular component with a root canal and a MB radicular component with only one root canal placed in a buccal position (Fig. 8). An extensive discussion of the evolution of the premolar roots and the peculiar aspect of the TD6.2 P_3 root complex may be read in Wood et al. (1988) and Bermúdez de Castro et al. (1999a).

As in the OES, the occlusal contour of the EDJ is asymmetric due to the distolingual protrusion of the talonid (Fig. 6). The tips of the main cusps are mesially displaced with regard to the external contour, and the tip of the lingual one is mesially displaced with regard to the tip of the buccal one. The buccal and lingual cusps are connected by a high continuous transverse crest.

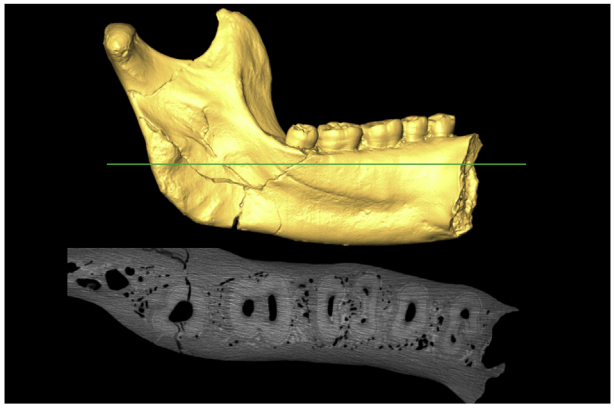

Figure 8. Virtual image of the mandible ATD6-96, showing a transversal section of the teeth at the root level. The images are not scaled.

The geometric morphometric study carried out by Gómez-Robles et al. (2008) clearly differentiated a primitive from a derived morphology of the crown contour. The primitive contour is observed in *Australopithecus*, *Paranthropus*, and early hominins, like *H. habilis*, *H. erectus* s.l., and *H. antecessor*, whereas the derived one is commonly found in Middle and Late Pleistocene hominins, including *H. sapiens*. The primitive pattern includes a marked to strongly pronounced asymmetrical outline, with a protruding distolingual contour. The lingual cusp is smaller than the buccal one and it is mesially displaced. The talonid is well developed and usually presents accessory tubercles and a more or less conspicuous cingulum. The two cusps are frequently connected by a transverse crest or separated by a shallow fissure. The two P_3 from TD6.2 share the plesiomorphic pattern with, among others, the Zhoukoudian, Sangiran, OH 16, Tighenif, KNM-ER 992, KNM-ER 15000, and Arago 71 specimens (e.g., Wood, and Uytterschaut, 1987; Tobias, 1991; Bermúdez de Castro et al., 1999a; Gómez Robles et al., 2008; Martinón-Torres et al., 2012; Xing et al., 2018). This primitive pattern differs from the more symmetric outline found in later hominins, where both the talonid and the occlusal polygon are significantly reduced.

Gómez-Robles et al. (2008) examined the allometric variation among taxa for the shape of this tooth. They observed that small premolar crowns tend to have a circular and symmetrical outline combined with a compressed and lingually-located occlusal polygon, whereas larger premolars present strongly asymmetrical outlines as a consequence of a conspicuous and well-developed talonid. It is interesting that the two TD6.2 P_3 are different sizes (Table 3), but the shape is very similar.

The roots of the TD6.2 P_3 are primitive and uncommon, but not autapomorphic, since a similar morphology (even though somewhat more simplified) is observed in the Early Pleistocene right and left P_3 of ATE9-1 (Atapuerca-Sima del Elefante; Prado-Simón et al., 2011), and in the P_3 of the Atapuerca-SH mandible AT-173. A polymorphic variability of the P_3 root complex is observed within the genus *Homo* (e.g, KGA 10–1, D2600, D211, the Zhoukoudian specimens PA110, ZKD21 ZKD23, ZKD82, ZKD85, Trinil 5, Lantian, or D211, the Sangiran specimens 5, 8, and 9, and Penghu 1), which can display from one root, to a Tomes' root type and two roots (2: MB + D; Weidenreich, 1937; Suwa et al., 2007; Martinón-Torres et al., 2008; Chang et al., 2014; Xing et al., 2018; also see Bermúdez de Castro et al., 1999a:Table 14, and references therein). A simplification of the P_3 root is observed in later hominins, like those of the Atapuerca-SH, *H. neanderthalensis* (see Genet-Varcin, 1962) and, of course, in *H. sapiens* (see Scott and Turner, 1997).

Lower fourth premolars (P_4): ATD6-4, ATD6-96, ATD6-125 ATD6-4 was described by Bermúdez de Castro et al. (1999a), and only a short note on the P_4 of ATD6-96 was written by Carbonell et al. (2005). ATD6-125 is unreported. This tooth is well preserved, except for the missing distal radical and the apex of the mesial radical of the root complex (Fig. 4). In ATD6-125 tooth wear has affected only the enamel (grade 2). The occlusal contour of the P_4 of ATD6-96 and ATD6-125 is a buccolingually elongated and asymmetric oval, with a distolingual protrusion. The lingual cusp is mesiodistally displaced with regard to the buccal cusp. In the P_4 of ATD6-96 and in ATD6-125 both cusps are connected by a continuous transverse crest (grade 2), whereas in ATD6-4 the connection is interrupted by the sagittal fissure (grade 1; Table 6). Between the mesial marginal ridge and the transverse crest there is an anterior fovea, particularly marked and deep in ATD6-4. In all cases, the metaconid is mesially displaced and there is a

conspicuous talonid where up to four accessory cusps develop (ATD6-4, ATD6-125, and ATD6-96). In ATD6-125, one of the accessory cusps occupies a remarkable distobuccal position within the talonid. The posterior fovea is conspicuous and adopts different shapes depending on the configuration of the crown. In ATD6-125, the posterior fovea is defined by the confluence of the sagittal groove, the groove separating the buccal cusp from the talonid, and the groove that differentiates the distolingual accessory tubercle of the talonid (Fig. 4). Two shallow vertical grooves, which are present in the buccal face of ATD6-125, define a vestige of cingulum, which is well marked in ATD6-4 (Bermúdez de Castro et al., 1999a).

The root of ATD6-4 is 2R: MB + DL, in which three root canals are present: a buccal, a distolingual, and a mesiolingual one (Bermúdez de Castro et al., 1999a). The root complex of ATD6-125 is formed by two radicals, mesial and distal, which diverge from around halfway along the root. A shallow groove runs along the mesial root from the cervical to the apical region. The P_4 of ATD6-96 shows a single root, with a broad canal.

At the EDJ level, we distinguish a mesially displaced and continuous transverse crest in all cases, although in ATD6-96 and ATD6-125 the crest is high and originates from the tip of the buccal cusp, and in ATD6-4 it is low and starts from a point mesial to the cusp tip (Fig. 6). This crest and the mesial marginal ridge enclose a remarkable anterior fovea in the three specimens. In ATD6-125 there is a clear ridge distal to the essential ridge that could correspond to a distal accessory ridge. The buccal surface exhibits two vertical grooves that define a vestige of a cingulum. Whereas, at the enamel, the talonid comprises several accessory cusps, these are barely distinguished at the level of the enamel.

The primitive morphology of the P_4 of the *Homo* clade includes a large talonid, which extends from the lingual to the buccal limits of the crown, as in the Dmanisi P_4 (Martinón-Torres et al., 2008). This molarized shape is also observed in *Australopithecus* (e.g., Sts 52, A.L. 333w-20), *H. habilis*, and *H. erectus* s.l. The distobuccal component of the talonid disappears in the European Pleistocene hominins, and is only restricted to the lingual half of the crown (Genet-Varcin, 1962; Patte, 1962, Martinón-Torres, 2006). This is the condition observed in ATD6-4 and in the P_4 of ATD6-96. However, in ATD6-125 the talonid exhibits the primitive condition, with both distolingual and distobuccal components. In general, the asymmetric contour, conspicuous talonid with accessory lingual cusps and the expression of a light cingulum provide a primitive conformation to the *H. antecessor* P_4. However, the occlusal polygon is reduced with regard to *H. habilis* and *H. erectus* s.l., falling close to Middle Pleistocene hominins with regards to this feature (Martinón-Torres, 2006).

On the other hand, the lack of a continuous transverse crest is considered the primitive condition for the genus *Homo,* as seen in *Australopithecus* (with the exception of A.L.-333w60 and A.L.-277-1), and African early *Homo* (*H. habilis*, and African *H. erectus*—e.g., OH7, OH 13, KNM.WT 15000, KGA 10–1; Tobias, 1991; Martinón-Torres et al., 2007; Suwa et al., 2007). In recent *H. sapiens* the crest is uncommon (Martinón-Torres et al., 2012). In contrast, a continuous transverse crest is characteristic of the European Middle Pleistocene hominins and the Neanderthals (Genet-Varcin, 1962; Bailey, 2002; Bailey and Lynch, 2005; Martinón-Torres, 2006; Martinón-Torres et al., 2007), and this is also frequent in fossil *H. sapiens* (Martinón-Torres et al., 2012), a well as in *H. erectus* from Sangiran (e.g., S6, S9). In Arago 13 and Arago 28 the transverse crest is interrupted by the sagittal fissure, but the crest is present in Arago 89. In the TD6 P_4 we observe a continuous transverse crest in two specimens, whereas ATD6-4 lacks this feature at the enamel.

The morphology of the ATD6-4 root complex may be a peculiarity of *H. antecessor*, although a similar morphology has been observed in Arago 13 (Bermúdez de Castro et al., 2018), Hexian (Liu et al., 2017) and Tighenif (Zanolli, 2013). The presence of mesial and distal roots (2R: M + D), like in ATD6-125, is also the most complex condition of the polymorphisms of the genus *Homo*, and it is observed in *H. habilis* and *H. erectus* s.l. (Weidenreich, 1937; Wood et al., 1988; Tobias, 1991; see also Bermúdez de Castro et al., 1999a:Table 14). The root of the left P_4 of the mandible ATE9-1 is classified as 2T (Wood et al., 1988) or grade 3 according to Turner et al. (1991). A single root is seen in the P_4 from Atapuerca-SH (Bermúdez de Castro, 1988; Martinón-Torres et al., 2012).

Lower first molars (M_1): ATD6-5, ATD6-94, ATD6-96, ATD6-112 The description of the M_1 of ATD6-5 was carried out by Bermúdez de Castro et al. (1999a). The rest of the M_1 sample has been mentioned in some previous reports (Carbonell et al., 2005; Bermúdez de Castro et al., 2010), but their morphology has never been published in detail. The M_1 of the immature mandible ATD6-112 has been virtually extracted (Bermúdez de Castro et al., 2010), and it is at stage D of the Demirjian et al. (1973) classification (Fig. 2). This tooth is unworn. The isolated M_1 of ATD6-94 (Fig. 4) shows a minimal wear in the enamel of the highest region of the crown (grade 2). The mesial root length of ATD6-94 is 9.0 mm and the distal root length is 8.0 mm (Bermúdez de Castro et al., 2010). The root length is approximately similar to the crown height (state F of the Demirjian et al., 1973 classification). In the M_1 of ATD6-96 (Fig. 9), all the cusps exhibit dentine patches (grade 3), with the largest one being observed at the protoconid.

The occlusal contour of all TD6.2 M_1s is a mesiodistally elongated and rounded rectangle. All M_1 show the main five cusps well integrated into the external contour of the tooth, and arranged in a clear Y-pattern in ATD6-5, ATD6-94, and ATD6-96 (Table 6). In ATD6-112, the main cusps are arranged in a cruciform (+) pattern. The hypoconulid is large (grade 4) or very large (grade 5), particularly in ATD6-96 and ATD6-112. This cusp occupies a central position, slightly buccally displaced along the distal margin in ATD6-5, ATD6-94, and ATD6-96 and with a clear distobuccal protrusion in the case of ATD6-112. A small metaconulid (C7) of grade 2 is present in ATD6-94. This tooth also expresses a moderate entoconulid (C6) of grade 2. ATD6-94 and ATD6-112 show an extensively crenulated occlusal surface, with numerous ridges and grooves. In all M_1 the anterior fovea has the shape of a short deep fissure and is delimited by a thick mesial marginal ridge and by the essential ridges of the protoconid and metaconid. These ridges form a mid-trigonid crest, which is continuous (grade 2) in only one of the four M_1 (ATD6-112; Martínez de Pinillos et al., 2017). In ATD6-94, the sagittal groove cuts the thick mesial marginal ridge. A distal trigonid crest, also interrupted by the central groove (grade 1), is also present in all M_1 (Martínez de Pinillos et al., 2017). A deflecting wrinkle (grade 2) is

Figure 9. Occlusal view of the molars of the mandible ATD6-96.

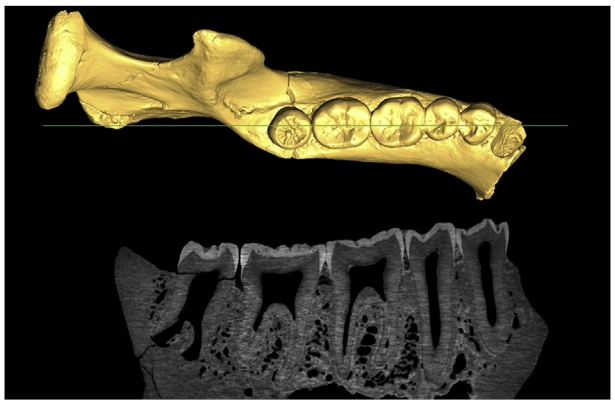

Figure 10. Virtual reconstruction of the mandible ATD6-96, showing a parasagittal cut at the level of the molars. Taurodontism increases progressively from M_1 to M_3. The images are not scaled.

present in ATD6-5 and ATD6-94. The protostylid is absent in all the TD6.2 M_1.

The μCT images of ATD6-5, ATD6-94, ATD6-96 reveal the amplitude of the pulp cavity and point to hypotaurodontism (Fig. 10), according to Shaw (1928) classification. In ATD6-94, we can take direct measurements of the root, and the divergence of the mesial and distal roots occurs about 4.0 mm from the cervical line.

With regard to the dentine (see Martínez de Pinillos et al., 2017:Figs. 4 and 6), no traces of deflecting wrinkle, talonid crest or protostylid are found, although ATD6-112 presents a marked groove in the buccal surface. This molar is the only M_1 that shows a continuous trigonid crest (type 10 of Martínez de Pinillos et al., 2014) that, together with the mesial marginal ridge, delimit a linear-like anterior fovea. The hypoconulid is large in all the M_1, and only ATD6-94 exhibits a small metaconulid and an entoconulid that has the aspect of a dentine wrinkle. Whereas the dentine surface of ATD6-5 and ATD6-96 is relatively simple, the surface of ATD6-94 and ATD6-112 is crenulated with grooves and accessory ridges in the main cusps, but never reaching the complexity of the dendrite-like pattern observed in Chinese classic *H. erectus,* like Zhoukoudian (PA 69) and Xichuan PA 531 (Xing et al., 2018).

The presence of the main five cusps in the M_1 is constant in the fossil record, with large or very large hypoconulids. The absence of this cusp is exceptional, and has been reported in the specimens AT-14 and AT-561 from the Atapuerca-SH dental sample (Bermúdez de Castro, 1993). The lack of hypoconulid is also infrequent in archaic and recent modern *H. sapiens* (Martinón-Torres et al., 2012). Regarding the expression of accessory cusps in early *Homo* and *H. erectus* s.l. the prevalence of these cusps, particularly the C7, is high and can be found in specimens like D211, D2735, OH 4, OH 7, OH 13, KNM-ER 992, KNM-WT 15000, ZKD 35, ZKD 36, and S7-42, S7-43, S7-62, and MA 93 (if this tooth is an M_1), as well as in Arago 13, Arago 89 and some specimens of the Atapuerca-SH M_1 sample. The prevalence of this cusp decreases in *H. neanderthalensis* and *H. sapiens* (Axelson and Kirveskari, 1979; Martinón-Torres et al., 2012). The C6 is somewhat less frequent in early hominins, and its expression is variable. Thus, the C6 is present in OH 4, OH 7, D 211, KNM-ER 992, and the Sangiran *H. erectus* (S5, S6, S7-20, S7-42, S7-62), as well as in some Neanderthals. In contrast, the C6 is absent in the Atapuerca-SH hominins, in African *H. erectus* s.l. (e.g., MA 93) or in the Zhoukoudian M_1 sample. Furthermore, the Y-groove pattern and the presence of secondary ridges and grooves (crenulations) is the primitive condition in *Australopithecus* and early *Homo*. All the unworn TD6.2 M_1 show crenulated enamel surfaces, but the EDJ does not reach the level of complexity described in *H. erectus* s.s. (Xing et al., 2014, 2016, 2018). ATD6-112 shows a cruciform grove pattern, a derived condition that is more commonly found from the Middle Pleistocene onwards, particularly in Eurasia (Martinón-Torres et al., 2007) with the exception of the Dmanisi sample (Martinón-Torres et al., 2008). This feature has been also observed in MA 93 from Buia (Zanolli et al., 2014). In other features, such as the large, buccally placed, and protruding hypoconulid, ATD6-112 would match the primitive condition expressed by *Australopithecus*, *H. habilis* (OH 7, OH 13, OH 16), and some *H. erectus* s.l. (D 211, D2735, KNM-WT-15000), and in some Zhoukoudian and Sangiran specimens.

A high prevalence of the deflecting wrinkle has been reported in the M_1 of some modern human populations (Axelson and Kirveskari, 1977). However, this feature does not have a clear pattern of distribution in fossil hominins. It is present in some specimens, like D211, KNM-WT 15000, in some M_1 of the Atapuerca-SH and Sangiran samples (Martinón-Torres et al., 2008, 2012), to which we can add ATD6-5 and ATD6-94. None of the specimens from Buia and Tighenif exhibits this morphological trait (Zanolli, 2013; 2014). A well-developed distal trigonid crest (see Scott and Turner, 1997) is another variable feature, without a clear pattern among fossil hominins. It has been described in D211, D2735, Sangiran 6, Sangiran 7–43, Xichuan PA531, Xujiayao PA1500, Hexian PA831 and in some Atapuerca-SH specimens (Martinón-Torres et al., 2008). In addition, the expression of this feature may be obscured by the presence of the deflecting wrinkle, a conspicuous metaconid essential ridge or a C7 (Martinón-Torres et al., 2008).

Although the presence of some morphological features, like the rounded and lobulated main cusps and the presence of additional cusps and ridges, may help to distinguish the M_1 of archaic hominins from later humans and particularly from recent *H. sapiens*, the majority of these features are of little significance in taxonomic or phylogenetic studies. However, the morphology of the anterior fovea is a remarkable tool for the identification of some taxa. Thus, in *Australopithecus*, *H. habilis*, and African *H. erectus* the anterior fovea is formed by a triangular depression that coalesces with the mesial marginal ridge and is distally bounded by the mesial aspects of the protoconid and the metaconid (Hrdlicka, 1924; Scott and Turner, 1997). This morphology is also observed in some Atapuerca-SH specimens and some Neanderthals, and it is the predominant type in fossil and recent *H. sapiens*. In contrast, this classic morphology differs from the deep fissure or pit-like fovea bounded by a high and thick mesial marginal ridge and a continuous or discontinuous mid-trigonid crest, usually found in Eurasian fossils like the Sangiran specimens S6, S7-20, S7-43, S7-61, S7-62, S7-76, NG8503, and MA 93 from Mulhuli-Amo (if we classify it as an M_1), most Atapuerca-SH M_1 and Neanderthals, as well as in Montmaurin, Arago 13, Arago 40, Arago 89 and MA 93 (Zubov, 1992; Bailey, 2002; Kaifu et al., 2005a,b; Martinón-Torres, 2006; Martínez de Pinillos et al., 2014; Zanolli et al., 2014). A continuous mid-trigonid crest is also present in the M_1 of MA 93, D211 and D2735, although the morphology of the anterior fovea resembles that of African contemporaneous populations (Martinón-Torres et al., 2008). The Zhoukoudian M_1 sample also lacks a mid-trigonid crest, except in ZKD34 (Xing et al., 2018). A mid-trigonid crest is also identified in Xichuan PA531 whereas it is absent in African *H. erectus* (Xing et al., 2018). Interestingly, the M_1 of the Mauer mandible (the holotype of *H. heidelbergensis*) and Mala Balanica specimen lack anterior fovea and a mid-trigonid crest. According to Zanolli and Mazurier (2013), the left M_1 of Tighenif 2 shows a continuous mid-trigonid crest at the enamel and dentine. However, unlike ATD6-112, this crest corresponds to a grade 2 according to Bailey et al. (2011), since the height of the crest is relatively reduced by the sagittal groove. The TD6.2 M_1 are therefore aligned with the Eurasian pattern by the morphology of the

anterior fovea and the presence (albeit interrupted except for ATD6-112) of a mid-trigonid crest.

The taxonomic value of this feature has been also revealed by the geometric morphometric analysis carried out by Gómez-Robles et al. (2015). This tooth is morphologically very stable, and the first two principal components (PC1 and PC2) of the relative warp analysis account for only 32.78% of total morphological variance and are not useful to distinguish among taxa. However, the PC3 (10.0% of the total variance) is able to distinguish the specimens with a mesiodistally elongated shape, a well-developed hypoconulid, a cruciform pattern, and a mesial displacement of the anterior fovea, originated by the presence of a well-defined mid-trigonid crest. Positive values of this component group and differentiate the European Middle Pleistocene hominins and the Neanderthals from other hominins (Gómez-Robles et al., 2015). Interestingly, the specimens ATD6-5, ATD6-94, and ATD6-96 cluster together in a region tangential to this group. The M_1 of ATD6-112 was not included in this study.

The absence of a protostylid in the M_1 from TD6.2 could be interpreted as a derived condition, considering that this feature is frequent in early hominins, like those of Hexian and Yiyuan (see Martinón-Torres et al., 2008, and references therein; Xing et al., 2014; 2016; Liu et al., 2017). However, the variable presence of the protostylid in recent *H. sapiens* (e.g., Dahlberg, 1950) prevents us from making a robust taxonomic evaluation of this feature.

Lower second molars (M_2): ATD6-5, ATD6-96, ATD6-113, ATD6-144 The description of the M_2 of ATD5 was written by Bermúdez de Castro et al. (1999a). Only some notes on the M_2 of ATD6-96 were reported by Carbonell et al. (2005), and a short description of the M_2 of ATD6-113 can be found in Bermúdez de Castro et al. (2008). Except for the analysis of the mid-trigonid crest expression at the EDJ (Martínez de Pinillos et al., 2017), ATD6-144 is unreported (Fig. 4). This tooth is unworn and reached state E of the Demirjian et al. (1973) classification. As in the other TD6.2 M_2, the occlusal contour is a rounded rectangle, mesiodistally elongated. All the TD6.2 M_2 exhibit the five main cusps, well integrated in the body of the tooth and arranged in a Y-pattern (Table 6). The hypoconulid is large or very large (grades 4 and 5), and occupies a central (ATD6-113, ATD6-94, ATD6-5) or more buccodistal position (ATD6-144). The presence of a C7 is conspicuous in ATD6-5 (grade 3). ATD6-144 could also present a C7 of grade 2, but the extensive crenulations of the occlusal surface hamper its identification. The C6 is absent in the sample. The deflecting wrinkle is absent in all M_2. The occlusal surface of ATD6-144 is complicated by several crenulations (secondary ridges and grooves). In particular, the essential ridge of the hypoconid shows a considerable development and forms an independent central cusp in contact with the other main cusps. In ATD6-5, the mesial ridge of the hypoconid is well developed, also producing an outstanding relief in the center of the occlusal surface.

The anterior fovea is deep and fissure-like in all M_2, and delimited by a thick mesial marginal ridge (especially conspicuous and crenulated in ATD6-144) and the mid-trigonid crest. This crest is continuous (grade 2) in two of the four M_2 (ATD6-5 and ATD6-113). The distal trigonid crest is invariably interrupted by the central groove. The protostylid is absent in all the TD6.2 M_2.

When observed with μCT, the images of ATD6-5 and ATD6-96 point to mesotaurodontism (Fig. 10) and hypotaurodontism in the case of ATD6-113.

Concerning the inner morphology of the M_2 (see Martínez de Pinillos et al., 2017:Figs. 4 and 6), ATD6-96 and ATD6-113 exhibit a small depression in the buccal surface of the protoconid that could be related to the lowest degree of protostylid expression. The specimens display the five main cusps with a Y-pattern configuration and a medium-sized hypoconulid, except for ATD6-144 where the C5 looks small. ATD6-5 is the only M_2 that expresses a metaconulid (C7), which is medium-sized. The occlusal surface of the ATD6.2 M_2 exhibits a discontinuous mid-trigonid crest with a discontinuous distal trigonid crest (type 4), so there is a discrepancy between the OES and the EDJ in three of the four specimens (Martínez de Pinillos et al., 2017).

The TD6.2 M_2 show a primitive morphology, well defined by the presence of the five main cusps arranged in a Y-pattern and the extensive crenulations of the occlusal surface. Along the evolution of the genus *Homo,* the reduction or lack of the hypoconulid also implies the reduction of the MD dimension. This fact is remarkable in the M_2 sample from Atapuerca-SH, in which one-third of the specimens lack the hypoconulid. This cusp is very small (grade 1) in Arago 13, and it is difficult to differentiate from the hypoconid in Arago 6. The C5 is absent in two of the 23 Neanderthal specimens examined by Martinón-Torres et al. (2012), and it is the most frequent situation in archaic and recent *H. sapiens*. The hypoconulid is also absent in the four M_2 identified by Zanolli (2013) from the Kabuh Formation of the Sangiran Dome (Central Java), attributed to *H. erectus*. The absence of the hypoconulid and the concomitant reduction of the MD dimension are captured by the geometric morphometric analysis carried out by Gómez-Robles et al. (2015). The three TD6.2 M_2 included in this analysis (ATD6-5, ATD6-96, and ATD6-113) occupy an extreme position in the negative region of the PC1 of the relative warp analysis, close to KNM-ER 992, Arago 10, Arago 89, OH13, and some *Paranthropus* specimens. The cruciform and X-groove pattern are also associated with the reduction of the hypoconulid in the analysis carried out by Gómez-Robles et al. (2015), as is observed in *H. sapiens*, in the Atapuerca-SH M_2, in the sample of *H. erectus* studied by Zanolli (2013), as well as in Sangiran 22, S7-64, and S7-45 (Martinón-Torres et al., 2008). It is interesting to note the buccolingual expansion of the mesial cusps in the classic *H. erectus* from Yiyuan, Hexian and Zhoukoudian (Weidenreich, 1937; Xing et al., 2014, 2016, 2018), a feature that is absent in the TD6.2 M_2.

The deflecting wrinkle is relatively frequent in the M_2 of *Australopithecus*, *H. habilis* (OH 16) and *H. erectus* s.l. (e.g., D211, KNM-WT 15000, KNM-ER 992, S7-62, S7-65, KNM-BK7905, SB8103, NG 8503, ZKD 107, ZKD 108, Yiyuan Sh.y.072, Hexian PA838 and PA839; Martinón-Torres et al., 2008; Xing et al., 2014, 2016) so it is likely a primitive feature. However, as in the M_1, the variability of this dental trait in *H. sapiens* (e.g., Hanihara et al., 1964; Sakuma et al., 1987) prevents us from drawing conclusions on its diagnostic value.

The deep pit or fissure-like fovea, delimited by the thick mesial marginal ridge and the mid-trigonid crest (interrupted or not), is very frequent in the Atapuerca-SH hominins, other European Middle Pleistocene hominins like Montmaurin and some Arago specimens (Arago 10, Arago 32, Arago 68), and the Neanderthals, but infrequent in Pleistocene African specimens (except in MA 93) and in the archaic and recent *H. sapiens* (Martinón-Torres et al., 2012). According to these authors, 66.6% of the Neanderthals and 71.4% of the Atapuerca-SH M_2 show the concomitant expression of a deep pit or fissure-like fovea and a continuous mid-trigonid crest. Therefore, this combination has been considered a derived characteristic of these hominins (Bailey, 2002; Martinón-Torres et al., 2007). Exceptions to this pattern are KNM-ER 1808, D2735, Sangiran 9, and PA70 from Zhoukoudian (Xing et al., 2018). In Arago 13 and Arago 89, as well as in ATD6-144, the mid-trigonid crest is interrupted by the central fissure, whereas in ATD6-5, ATD6-96 and ATD6-113 this crest is continuous at the enamel but discontinuous at the dentine. This lack of correlation between the expression of the mid-trigonid crest in both surfaces is also observed in the left M_2 from Tighenif 1 and Tighenif 2, whereas the right M_2 of Tighenif 1 shows a continuous mid-trigonid crest at the enamel and dentine but its height is considerably reduced. The anterior fovea and the

mid-trigonid crest are absent in the M_2 of the Mauer and Mala Balanica mandibles. A mesially located anterior fovea is also captured by the PC2 of the morphometric analysis carried out by Gómez-Robles et al. (2015) in most Neanderthals, Atapuerca-SH specimens, Arago 10, Arago 13, Arago 89, and the TD6.2 M_2, among others. The distal trigonid crest is less frequent in hominins, except for the *H. neanderthalensis* sample studied by Martinón-Torres et al. (2012), so the taxonomic significance is limited.

The root complex of the TD6.2 M_2 is very different from the particularly robust morphology of the Penghu 1 specimen (Chang et al., 2014). Taurodontism has been considered as a frequent feature of Neanderthals (e.g., Blumberg et al., 1971; Kricun et al., 1999; Bailey, 2002, 2004; 2006; Kupczik and Hublin, 2010). However, this feature is also common in other Pleistocene hominins. Thus, the Asian *H. erectus* M_2 is characterized by having stout roots and some degree of taurodontism (Weidenreich, 1937), which according to Xing et al. (2018), could be a mechanism to withstand high biomechanical demand. According to Benazzi et al. (2015), taurodontism should be considered either an adaptation to a diet which implies a high attrition or, most likely, the result of pleiotropic or genetic drift effects.

The EDJ surface of the TD6.2 M_2 is relatively simple and smooth as in most hominins. In contrast, and as we have noted in other tooth classes, the classic *H. erectus* from Zhoukoudian (PA70), Hexian (PA839, PA831, PA834-1), Yiyuan (Sh.y.072), and Xichuan (PA532 and PA533) exhibit a complicated and derived dendrite-like pattern (Xing et al., 2014, 2016, 2018).

Lower third molars (M_3): ATD6-5, ATD6-96, ATD6-113 The M_3 has been virtually extracted from the immature mandible ATD6-5 (Bermúdez de Castro et al., 1999a), and it is between stage D and E of the Demirjian et al. (1973) classification. The root reaches a maximum length of 2.4 mm at the level of the distolingual aspect. Except for the analysis of the trigonid crest at the EDJ (Martínez de Pinillos et al., 2017), the morphology of this tooth is unreported. Regarding the M_3 of ATD6-96 only some aspects related to its size have been mentioned in Carbonell et al. (2005), but it is the first time that its OES and EDJ is reported. Finally, only a brief description of the M_3 of the mandible ATD6-113 (Bermúdez de Castro et al., 2008) and the trigonid crests (Martínez de Pinillos et al., 2017) has been published.

The occlusal contour of ATD6-5 (see Martínez de Pinillos et al., 2017:Figs. 4 and 6) is a mesiodistally elongated rectangle that tapers at the distolingual side. The five main cusps are arranged in a Y-pattern (Table 6). The hypoconulid is large (grade 4) and placed in a distobuccal position. A small C6 (grade 1) is present in this tooth and a large C7 (grade 4) is also expressed. The unworn occlusal surface exhibits secondary ridges and grooves, giving a complicated aspect to its surface. The essential ridges of the main cusps are well defined, except that of the metaconid, and a well-defined mid-trigonid crest is absent. The anterior fovea takes the form of a broad and long valley limited by a thin mesial marginal ridge and, in part, by the essential ridge of the protoconid. The sinuous central groove cuts both the mesial and distal trigonid crests. No signs of a deflecting wrinkle or protostylid are present in this tooth.

In contrast to the size and complexity of ATD6-5, the M_3 of ATD6-96 is very reduced in comparison with the M_1 and M_2 (Fig. 9), and it is difficult to identify the key elements of the tooth. Thus, the hypoconid is placed in the trigonid area of the molar and the distal cusps adopt a triangular shape with unclear limits. Because this tooth shows little occlusal wear (grade 2) it is possible to identify at least 12 successive ridges converging to the center of the occlusal surface. The more conspicuous ridge probably corresponds to the essential ridge of the entoconid, and forms a notable central tubercle. The hypoconulid is medium-size (grade 3) and the C6 is delimited by two grooves (grade 2). The anterior fovea may be defined by the most anterior depression, between the thick mesial marginal ridge and the most anterior two ridges. The protostylid is represented by a small pit (grade 1). The root complex of the M_3 of ATD6-96 is hypertaurodont (Fig. 10). The divergence of the two roots occurs only at the last one-third of their length. The roots remain open and they are at stage G of the Demirjian et al. (1973) classification.

The M_3 of ATD6-113 is well developed, exhibiting moderate occlusal wear (grade 2) and a crenulated occlusal surface. This tooth exhibits the five main cusps arranged in a Y-pattern. In this case, the hypoconulid occupies a more distal than buccal position. A small C6 is present. The deep and short fissure-like anterior fovea is bounded by the thick mesial marginal ridge and the continuous mid-trigonid crest (grade 2). There is a discontinuous distal trigonid crest. The secondary fissure differentiates two small tubercles between the entoconid and the hypoconulid at the distobuccal corner of the crown. The μCT images suggest that the M_3 of ATD6-96 is hypertaurodont (Fig. 10), whereas the M_3 of ATD6-113 shows mesotaurodontism.

Concerning the dentine surface, there is no expression of talonid crests or a deflecting wrinkle in all the TD6.2 M_3 (see Fig. 6 and Martínez de Pinillos et al., 2017). Only ATD6-113 exhibits a deep anterior fovea and a continuous mid-trigonid crest, a small hypoconulid and a C6 with the aspect of a low dentine wrinkle. ATD6-5 presents the five main cusps and a large C7 with a well-developed essential ridge. ATD6-96 shows a small pit in the buccal surface that could correspond to a protostylid. In contrast to what is seen in the enamel, the hypoconulid and the C6 appear as weak elevations in the occlusal rim.

It seems that the size reduction of the M_3 occurred during the Early Pleistocene. Despite its complex occlusal morphology, the size of D211 M_3 from Dmanisi is very small (Martinón-Torres et al., 2008). Therefore, the extreme size reduction of the M_3 of the mandible ATD6-96 (like the extreme reduction of the M^3 of the maxilla ATD6-69) is not surprising. The size reduction, together with the loss of the hypoconulid, would be a derived condition of the *Homo* clade, particularly apparent in the case of the Atapuerca-SH teeth (Bermúdez de Castro and Nicolás, 1995; Martinón-Torres et al., 2012), as well as in some Neanderthals. This trend has been also noted in the Chinese *H. erectus* (ZKD B2-64 and ZKD F1225; Weidenreich, 1937), and in the *H. erectus* specimens from the Kabuh Formation of the Sangiran Dome (Central Java; Zanolli, 2013). Furthermore, the congenital absence of the M_3 has been reported in Penghu 1 (Chang et al., 2014), and it is also a feature of the Lantian specimen (authors' pers. obs.). In consonance with this reduction, a change from the primitive Y-pattern to the X and cruciform patterns is also a relatively derived condition, a common pattern in the Middle Pleistocene (Weidenreich, 1937; Bermúdez de Castro, 1988; Martinón-Torres, 2006; Zanolli, 2013). The complicated topography of the occlusal surface of the TD6.2 M_3 is common (and plesiomorphic) in early hominins, as in OH 13, D211, Zhoukudian, and some Neanderthals (Weidenreich, 1937; Tobias, 1991; Martinón-Torres et al., 2008).

The ATD6-113 M_3 has a well-defined anterior fovea. This feature is very frequent in the European Middle Pleistocene hominins and the Neanderthals. Furthermore, the concomitant presence of an anterior fovea with a continuous mid-trigonid crest is characteristic of the Montmaurin M_3, Atapuerca-SH hominins (57.1%) and Neanderthals (64.7%), and is not uncommon in the Sangiran specimens (Martinón-Torres, 2006; Martinón-Torres et al., 2012). The anterior fovea is less frequent and conspicuous in *H. sapiens*, and is not distally bounded by the mid-trigonid crest. ATD6-113 and the left M_3 from Tighenif 1 show a continuous mid-trigonid crest, although the height of the latter is remarkably depressed. However, ATD6-5 and ATD6-96 exhibit an absent or discontinuous mid-trigonid crest.

This configuration is also present in the M_3 from Arago (Arago 106), Tighenif 1 (right M_3) and Tighenif 2.

The expression of a continuous distal trigonid crest has been described as more frequent in Neanderthals and their ancestors (Bailey et al., 2011; Martínez de Pinillos et al., 2014), but this feature is absent in the TD6.2 sample.

The geometric analysis carried out by Gómez-Robles et al. (2015) is not particularly discriminant, since there is an overlap among the different taxa given the large variability of this dental class. Those M_3 with large talonids are differentiated from the M_3 without a hypoconulid and reduction of the hypoconid and entoconid. In the positive values of the PC2 of the relative warp analysis of Gómez-Robles et al. (2015) we find specimens with a well-developed mid-trigonid crest and an associated mesial displacement of the anterior fovea. In this region of the morphospace, we find the Atapuerca-SH hominins, Arago 13, ATD6-113, and some Neanderthals, as well as the specimens assigned to *Paranthropus boisei*. It is interesting that the Atapuerca-SH hominins are well differentiated from modern humans, despite the size reduction in both cases. The Atapuerca-SH hominins have a relatively reduced buccolingual dimension, as well as centrally compressed cusp apices, a feature shared with ATD6-113. The extremely reduced M_3 of ATD-96 represents one of the exceptions observed so far in the Early Pleistocene hominins.

At the EDJ, ATD6-5 exhibits a well-marked C7. The M_3 of Tighenif 2 also shows a C7, as well as a C6. These additional cusps are not present in the M_3 of Tighenif 1. The dendrite-like EDJ surface is observed in the M_3 PA831 and PA834-2 from Hexian (Xing et al., 2014), thus confirming that this derived pattern is characteristic of the classic *H. erectus* from Hexian, Zhoukoudian, and Yiyuan (Xing et al., 2018).

4. Discussion and conclusions

Through the description of the TD6.2 permanent teeth we show that these hominins exhibit a combination of primitive and derived features with regard to the genus *Homo*. Several authors have investigated the mechanisms behind the mosaicism in the dentition. From a systematic geometric morphometric analysis of the TD6.2 premolars and molars, Gómez-Robles et al. (2015) concluded that most of the features of the mandibular dentition of *H. antecessor* were plesiomorphic, whereas the maxillary dentition was more derived, showing a higher resemblance to the Neanderthal species. According to Gómez-Robles et al. (2015), these results probably reflect the stronger integration and more static pattern of evolution undergone by the mandibular dentition, whereas the opposite may be characteristic of the maxillary dentition (Gómez-Robles and Polly, 2011). Although a certain degree of coevolution is expected between teeth and jaws (e.g., Plavcan and Daegling, 2006; Boughner and Hallgrímsson, 2008), Gómez-Robles and Polly (2011) considered that the differences in the strength of integration between the maxillar and the mandible could be related to different anatomical constraints. For these authors, the more stable environment of the mandible could facilitate a high integration of the lower teeth, whereas the maxillary dentition is more sensitive to the strong evolutionary changes in the cranium and in the face, leading to a weaker integration of the upper teeth.

These patterns can be explained by the modular nature of the dentition and its evolution in mosaic (Klingenberg, 2008). In fact, the dentition as a whole constitutes a developmental module partially independent from other skeletal related parts (Stock, 2001), although the precise degree of genetic and phenotypic independence is still a matter of research (e.g., Butler, 1995; Stock, 2001; Miller et al., 2007, and references therein). Furthermore, the presence of different modules within the dentition has been postulated, apparently following different pathways. Thus, the anterior teeth seem to follow different evolutionary size changes with regard to the postcanine dentition in both modern humans and fossil hominins (e.g., Mizoguchi, 1981; Kieser and Groeneveld, 1987; Kieser, 1990; Bermúdez de Castro, 1993; Martinón-Torres et al., 2007). Although Gómez-Robles and Polly (2011) have found a significant covariation between premolars and molars, suggesting no modularization of premolar and molar fields, quantitative genetic studies have postulated the existence of a premolar module that has incomplete pleiotropy with the molar module (Hlusko and Mahaney, 2009; Hlusko et al., 2011). The latter would be in line with the different evolutionary trends ascertained in the morphology of the premolars in several hominin species, including *H. antecessor* (Martinón-Torres, 2006; Gómez-Robles et al., 2008).

It is important to acknowledge that late Early Pleistocene hominins from Europe retained a significant suite of plesiomorphic dental features, even if these primitive features have limited utility to elucidate their phylogenetic relationships. Some of these primitive features are the asymmetric crown, a buccal cingulum vestige, and complex root system of lower premolars with an expanded occlusal polygon in the case of the P_3, complex, and crenulated occlusal and buccal surfaces in molars and premolars as well as the M1 < M2 sequence in all molar specimens (see Fig. 11 for a comparative illustration of some of these traits). Although the crown shape of the TD6.2 upper premolars, especially the P^4, is nearly symmetric and the lingual cusp is proportionately reduced in comparison to the buccal one, these teeth still retain a vestige of a buccal cingulum, several crenulations at the buccal surface, conspicuous essential ridges and wide and robust root systems. These traits are common in most of the Early and Middle Pleistocene hominins from Africa such as *H. habilis*, *H. ergaster* and the Buia and Tighenif specimens.

The identification of primitive features in the mandibular and dental evidence was the main reason to propose a direct relationship between African *H. erectus* and *H. antecessor* (Carbonell et al., 1995; Bermúdez de Castro et al., 1997) back in the 1990s. However, the identification of some features in the TD6.2 sample that are present in Asian *H. erectus* but are absent in contemporaneous African populations has brought this hypothesis into question. The ascription of the *H. antecessor* teeth to a Eurasian dental pattern (Martinón-Torres, 2006; Martinón-Torres et al., 2007) suggests an early differentiation of the Eurasian Early Pleistocene groups from their African counterparts that may have started soon after the first documented hominin colonization of Eurasia (Gabunia and Vekua, 1995). Among the features that cluster *H. antecessor* with the Eurasian groups we can highlight the morphology of TD6.2 anterior teeth. Although the TD6.2 anterior teeth sample is limited, both the maxillary and mandibular incisors show the characteristic Eurasian pattern, particularly in the combination of pronounced labial convexity and shovel shape in this dental class and an incipient triangular shovel shape in the TD6.2 I^2 (Martinón-Torres, 2006; Gómez-Robles, 2010; Fig. 11). Furthermore, the strong bulging of the upper part of the buccal surface of upper premolars is a derived trait within the genus *Homo,* characteristic of the Eurasian groups. Both the M^1 and M^2 display largely divergent roots that delimit an area of anchorage in the maxilla that is clearly greater than the crown area. This configuration may be an effective mechanism to dissipate the forces exerted during powerful mastication and has been observed in some Asian specimens like ZKD 33 and ZKD 95 (Weidenreich, 1937). Finally, the compressed occlusal polygon of P_4 together with the expression of a continuous transverse crest in most of the TD6.2 specimens (Martinón-Torres, 2006) reinforce the departure from the African *H. erectus* morphologies.

In relation to this, it is interesting to highlight the expression in TD6.2 of some features within the Eurasian dental pattern that will

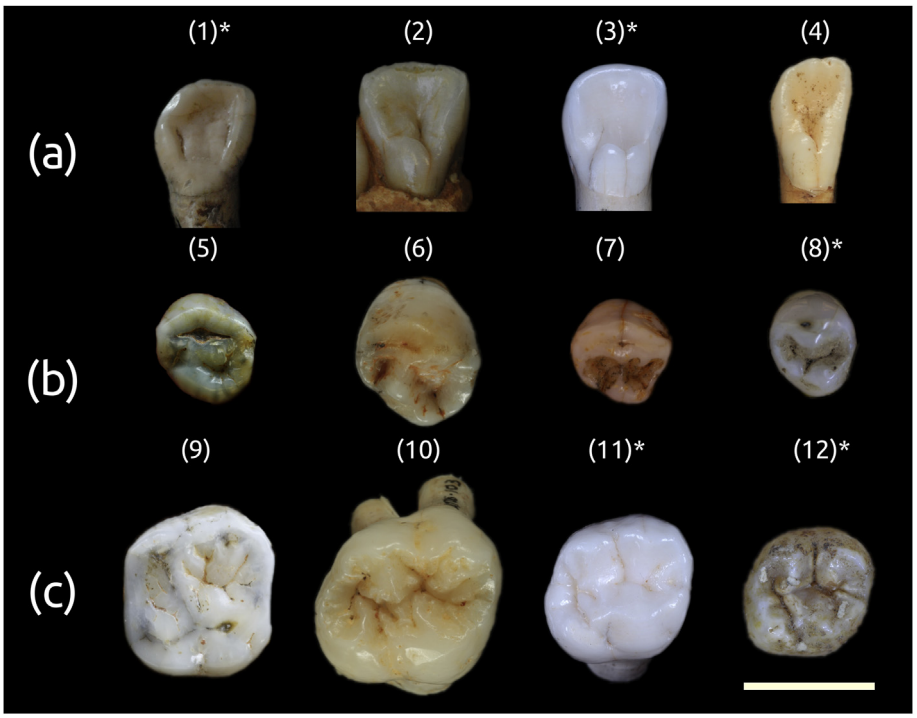

Figure 11. Comparative morphology of the lingual side of upper lateral incisors (a), occlusal view of lower third premolars (b), and occlusal view of upper first molars (c). 1 = Dmanisi D2677; 2 = Gran Dolina ATD6-69; 3 = Sima de los Huesos AT-1124; 4 = *Homo sapiens* from Maltravieso MTV 1418; 5 = Sangiran S7-25; 6 = Gran Dolina ATD6-3; 7 = *Homo neanderthalensis* from Hortus IV; 8 = *Homo sapiens* from Hayonim H19; 9 = *Homo erectus* from Chaoxian; 10 = Gran Dolina ATD6-103; 11 = Sima de los Huesos AT-2071; 12 = Qafzeh 11. Photographs denoted with an asterisk have been horizontally flipped to show the same side as Gran Dolina teeth. Scale bar = 10 mm.

be retained by the European Middle Pleistocene hominins, such as the Atapuerca-SH specimens, and that will become the typical condition of the Neanderthal species (Martinón-Torres et al., 2007; this study). These features highlight the deep chronological roots of the Neanderthal morphology and warn about the fact that some traits largely interpreted as Neanderthal apomorphies are indeed primitive features that appeared in the fossil record close to 1 Ma and became the typical Neanderthal pattern by an increase in the frequencies and degrees of expression. Among those, the concomitant presence of a fissure-like anterior fovea and a continuous mid-trigonid crest, typical of the Neanderthal lineage, is already present in the TD6.2 sample although at lower frequencies (Martínez de Pinillos et al., 2017). This combination is also present in the Dmanisi hominins (Martinón-Torres et al., 2008) although information on the EDJ is not available. This pattern is interpreted as the morphological base from which the typical Neanderthal morphology developed, with not only a continuous but a higher mid-trigonid crest than in the Early Pleistocene hominins (Bailey et al., 2011; Martínez de Pinillos et al., 2014, 2017). Concerning other skeletal parts, it is equally interesting to consider the size and shape of the clavicle (Carretero et al., 1999), the size and shape of the distal part of the humerus (Bermúdez de Castro et al., 2012), the presence of the medial pterygoid tubercle in the mandible (Bermúdez de Castro et al., 2014), as well as some other cranial features that reinforce the link of *H. antecessor* with Neanderthals and their ancestors (Arsuaga et al., 1999).

In this context, we suggest that TD6.2 hominins entered Europe probably after the Jaramillo event or perhaps before (Carbonell et al., 2008). The analysis of the ca. 1 Ma old specimens from Buia in Eritrea (Zanolli et al., 2014) points to some similarities with *H. antecessor* in the early expression of features such as a cruciform groove pattern and a continuous mid-trigonid crest, but the Buia incisors do not present the Eurasian signature of the TD6.2 specimens, suggesting that their separation may have occurred around 1 Ma or before. The origin of the TD6.2 hominins could be an ancient population living in Africa or perhaps in Southwest Asia, in the crossroad between both continents (see Bermúdez de Castro and Martinón-Torres, 2013; Bermúdez de Castro et al., 2017a). T his population would have already differentiated from the African Pleistocene *Homo* and would express some of the derived features later inherited by Neanderthals and their ancestors in the Middle Pleistocene, as well as by modern humans. This source population could have given rise to *H. sapiens* in Africa whereas in Eurasia it would have evolved towards the Neanderthal clade (Bermúdez de Castro and Martinón-Torres et al., 2013). The settlement of Europe may not have been necessarily linear and continuous, but may have been the result of several intermittent and successive dispersals from a source outside Europe, conditioned by the changing climatic conditions (Dennell et al., 2011; Bermúdez de Castro and Martinón-Torres et al., 2013; Bermúdez de Castro et al., 2016, and references therein). This pattern of discontinuous settlement could explain the high morphological variability of the European Pleistocene populations despite their phylogenetic link. In this scenario, we cannot discard the idea that some groups of *H. antecessor* may have persisted in southern Europe coexisting in time with later *Homo* groups.

Among the dental features that link *H. antecessor* with the Neanderthal lineage, it is important to highlight the derived shape of the M^1 (Fig. 11). TD6.2 hominins share with Neanderthals and most of their ancestors the expression of a rhomboidal occlusal polygon, the relative displacement of the lingual cusps and the protruding hypocone of the M.[1] This conformation has been seen so far only in the European Middle Pleistocene hominins and Neanderthals.

A possible explanation of the M^1 synapomorphy would be the direct in situ evolution of the Early Pleistocene hominins found in

Europe into the Neanderthal lineage. Despite the hard climatic oscillations in the continent during the Early and, particularly, the Middle Pleistocene periods (e.g., Dennell et al., 2011) the Iberian Peninsula may have been one of the most effective refugia of the whole European continent. The relatively abundant fossil record of Iberia during this period (e.g., Carbonell et al., 2008; Bermúdez de Castro et al., 1999a,b; Toro-Moyano et al., 2013; Bermúdez de Castro et al., 2017a; Daura et al., 2017) could be additional evidence of the potential role of Iberia as a speciation center and would explain the early presence of Neanderthal traits in the TD6.2 hominins, one of them (the derived shape of the M^1) not found so far outside Europe. However, this scenario seems less parsimonious and would imply a very early divergence of the Neanderthal and *H. sapiens* lineages.

Alternatively, the shape of the M^1 might have been polymorphic in the original population (i.e., with some specimens more derived than others) and later inherited by some (but not all) European Middle Pleistocene groups, becoming fixed in Neanderthals as one of its most characteristic features (Bailey, 2002; Gómez-Robles et al., 2008). As an example of this variability, the Arago dental sample exhibits a majority of plesiomorphic features, combined with some derived traits shared with Neanderthals (Bermúdez de Castro et al., 2003, 2018). The primitive aspect of the M^1 in this sample is remarkable, with an approximately square occlusal polygon and a regular contour in which no cusp protrudes on the external outline (Gómez-Robles et al., 2007). Interestingly, the Arago hominins also lack the modern features present in *H. antecessor* (Bermúdez de Castro et al., 1997; Arsuaga et al., 1999). In addition, we cannot rule out complex population dynamics and interactions underlining the great variability of the European hominin fossil record. This variability has been already interpreted as the result of the coexistence of different lineages in the continent (Tattersall, 2011; Martinón-Torres et al., 2012; Arsuaga et al., 2014; Bermúdez de Castro et al., 2018).

Another important aspect derived from the study of the teeth, and confirmed by the examination of other anatomical parts (Bermúdez de Castro et al., 1997; Arsuaga et al., 1999) is the differentiation of *H. antecessor* from the Asian *H. erectus.* For instance, TD6.2 upper and lower canines have lost the cingulum and associated structures, whereas these features are present at least in the Zhoukoudian and Yiyuan specimens (Weidenreich, 1937; Xing et al., 2016). In addition, the reduction of the lingual cusp and the occlusal polygon in the TD6.2 P^3 and the compressed occlusal polygon in the P_4 are also derived features in this sample with regard to the Asian hypodigm. The buccolingual expansion of the mesial cusps in the M_2 and M_3 of some classic *H. erectus* (Zhoukoudian, Hexian, and Yiyuan) seems to be a particularity of the Asian hominins and absent in TD6. Likewise, the dendrite-like pattern of the EDJ of the premolars and molars of some Chinese classic *H. erectus*, like Hexian, Zhoukoudian, Yiyuan, and Xichuan (Xing et al., 2014, 2016, 2018) has been found, so far, in only the Asian hypodigm and the only I^1 preserved in TD6 does not show the labial crenulations present in Hexian and Zhoukoudian (Xing et al., 2014, 2018). These features reinforce the idea that the TD6.2 hominins represent a European lineage, clearly divergent from the lineage formed by hominins attributed to the classic *H. erectus*, represented by paleodemes like Zhoukoudian, Yiyuan, Hexian, or Xichuan (Xing et al., 2018).

Finally, while *H. antecessor* shares some cranial and postcranial features with *H. sapiens*, the teeth, in particular, do not show any synapormophy with modern humans. The fact that TD6.2 teeth do not share any derived feature with *H. sapiens* warns about the possibility that the last common ancestor (LCA) may not display a 'neutral' or 'undefined' morphotype but, as is the case for the dentition, the LCA may display more Neanderthal-like features than *H. sapiens*-like (see Gómez-Robles et al., 2015 and Mounier and Mirazón Lahar, 2016 for discussion about the LCA morphology). Previous analysis of the hominin dental evidence from the Pleistocene revealed a relatively high number of autapomorphies in *H. sapiens* (Martinón-Torres et al., 2007), whereas the Neanderthal phenotype was built on the high frequencies and pronounced degrees of expression of plesiomorphic features.

Overall, the data presented here support the taxonomic validity of *H. antecessor*, since this species presents a mosaic of traits that is unique to this group. More than twenty years ago, *H. antecessor* was proposed as the best candidate to represent the LCA of modern humans and Neanderthals (Bermúdez de Castro et al., 1997). The fact that the paleogenetic studies were pointing to a more recent split for both lineages (Ovchinnikov et al., 2000; Ho et al., 2005; Green et al., 2010; Endicott et al., 2010; Krause et al., 2010; Reich et al., 2010; Meyer et al., 2016; but see Langergraber et al., 2012) was an important handicap for the acceptance by the scientific community of this phylogenetic hypothesis for the TD6.2 sample. The molecular study of the Sima de los Huesos hominins has led to the proposal of an earlier split for Neanderthals and modern humans (Meyer et al., 2016), so the genetic data are now compatible with the proposal of a split in the late Early Pleistocene/early Middle Pleistocene. Currently, TD6.2 hominins represent the best opportunity to infer the morphology of the last common ancestor (Bermúdez de Castro et al., 2018) although more fossil evidence is needed in order to have a more precise picture of the scenario.

Summarizing, the evidence presented in this study is compatible with previous hypothesis about the TD6.2 hominins (Bermúdez de Castro et al., 1997, 2018 and references therein). This evidence suggests that *H. antecessor* could belong to the basal populations from which other populations such as *H. sapiens*, *H. neanderthalensis* and Denisovans emerged. Future findings and additional research may help to elucidate the precise phylogenetic link among them.

Acknowledgements

Without the effort of the members of the Atapuerca Research Team during fieldwork, this work would have not been possible. We would like to make a special mention to the contribution of Jaume Guiu, who is deeply missed. This report has been mainly supported by the Dirección General de Investigación of the Spanish Ministry of Economy and Competitiveness (MINECO/FEDER), grant numbers CGL 2015-65387-C3-2, 3-P; and the Consejería de Cultura y Turismo of the Junta de Castilla y León, by the British Academy International Partnership and Mobility International Fellowship (PM160019). We also acknowledge The Leakey Foundation through the personal support of Gordon Getty (2013) and Dub Crook (2014, 2015, 2016, 2018) to one of the authors (M.M.-T.), and to the Atapuerca Foundation for their postdoctoral grant to M.M.-P. C.G.-C. and M.M.-M. are funded by a doctoral grant from the European Social Funds (BOCYL-D-30122013-33) through the Consejería de Educación de Castilla y León (Spain). L.M.-F. received financial support from the French State as part of the 'Investments for the future' Programme IdEx Bordeaux, reference code ANR-10-IDEX-03-02. The μCT images were obtained in the Laboratory of Microscopy of the CENIEH-Instalación Cientifico Técnica Singular (ICTS) (Spain) in collaboration with CENIEH staff. Restoration and conservation works on the material have been carried out by Pilar Fernández-Colón and Elena Lacasa from the Conservation and Restoration Area of CENIEH-ICTS and Lucía López-Polín from Institut Català de Paleoecologia Humana i Evolució Social (IPHES). We also acknowledge three anonymous reviewers, the Editor and the Associate Editor for valuable comments and revisions that have helped to improve the manuscript.

Supplementary Online Material

Supplementary online material to this article can be found online at https://doi.org/10.1016/j.jhevol.2018.12.001.

References

Álvarez-Posada, C., Parés, J.M., Cuenca-Bescós, G., van der Made, J., Rosell, J., Bermúdez de Castro, J.M., Carbonell, E., 2018. A post-Jaramillo age for the artefact-bearing layer TD4 (Gran Dolina, Atapuerca): New paleomagnetic evidence. Quaternary Geochronology 45, 1–8.

Arnold, L.J., Demuro, M., 2015. Insights into TT-OSL signal stability from single-grain analyses of known-age deposits at Atapuerca, Spain. Quaternary Geochronology 30, 472–478.

Arnold, L.J., Demuro, M., Parés, J.M., Pérez-González, A., Arsuaga, J.L., Bermúdez de Castro, J.M., Carbonell, E., 2015. Evaluating the suitability of extended-range luminescence dating techniques over early and Middle Pleistocene time-scales: Published datasets and case studies from Atapuerca, Spain. Quaternary International 389, 167–190.

Arsuaga, J.L., Martínez, I., Lorenzo, C., Gracia, A., 1999. The human cranial remains from Gran Dolina Lower Pleistocene site (Sierra de Atapuerca, Spain). Journal of Human Evolution 37, 431–457.

Arsuaga, J.L., Martínez, I., Arnold, L.J., Aranburu, A., Gracia-Téllez, A., Sharp, W.D., Quam, R.M., Falguères, C., Pantoja-Pérez, A., Bischoff, J., Poza-Rey, J., Parés, J.M., Carretero, J.M., Demuro, M., Lorenzo, C., Sala, N., Martinón-Torres, M., García, N., Alcázar de Velasco, A., Cuenca-Bescós, G., Gómez-Olivenza, A., Moreno, D., Pablos, A., Shen, C.-C., Rodríguez, L., Ortega, A.I., García, R., Bonmatí, A., Bermúdez de Castro, J.M., Carbonell, E., 2014. Neandertal roots: Cranial and chronological evidence from Sima de los Huesos. Science 344, 1358–1363.

Axelson, G., Kirveskari, P., 1977. The deflecting wrinkle on the teeth of Icelanders and the Mongoloid dental complex. American Journal of Physical Anthropology 47, 321–324.

Axelson, G., Kirveskari, P., 1979. Sixth and seventh cusp on lower molar teeth of Icelanders. American Journal of Physical Anthropology 51, 79–82.

Bailey, S.E., 2002. A closer look at Neanderthal postcanine dental morphology: the mandibular dentition. Anatomical Record 269, 148–156.

Bailey, S.E., 2004. A morphometric analysis of maxillary molar crowns of Middle-Late Pleistocene hominins. Journal of Human Evolution 47, 183–198.

Bailey, S.E., 2006. Beyond shovel-shaped incisors: Neandertal dental morphology in a comparative context. Periodicum Biologorum 108, 253–267.

Bailey, S.E., Lynch, J.M., 2005. Diagnostic differences in mandibular P4 shape between Neandertals and anatomically modern humans. American Journal of Physical Anthropology 126, 268–277.

Bailey, S.E., Skinner, M.M., Hublin, J.-J., 2011. What lies beneath? An evaluation of lower molar trigonid crest patterns based on both dentine and enamel expression. American Journal of Physical Anthropology 145, 505–518.

Benazzi, S., Nguyen, H.N., Kullmer, O., Hublin, H.-H., 2015. Exploring the biomechanics of taurodontism. Journal of Anatomy 226, 180–188.

Berger, G.W., Pérez-González, A., Carbonell, E., Arsuaga, J.L., Bermúdez de Castro, J.M., Ku, T.L., 2008. Luminescence chronology of cave sediments at the Atapuerca paleoanthropological site, Spain. Journal of Human Evolution 55, 300–311.

Bermúdez de Castro, J.M., 1986. Dental remains from Atapuerca (Spain) I. Metrics. Journal of Human Evolution 15, 265–287.

Bermúdez de Castro, J.M., 1988. Dental remains from Atapuerca/Ibeas (Spain) II. Morphology. Journal of Human Evolution 17, 279–304.

Bermúdez de Castro, J.M., 1993. The Atapuerca dental remains. New evidence (1987-1991 excavations) and interpretations. Journal of Human Evolution 24, 339–371.

Bermúdez de Castro, J.M., Martinón-Torres, M., 2013. A new model for the evolution of the human Pleistocene populations of Europe. Quaternary International 295, 102–112.

Bermúdez de Castro, J.M., Nicolás, E., 1995. Posterior dental size reduction in hominids. The Atapuerca evidence. American Journal of Physical Anthropology 96, 335–356.

Bermúdez de Castro, J.M., Arsuaga, J.L., Carbonell, E., Rosas, A., Martínez, I., Mosquera, M., 1997. A hominid from the Lower Pleistocene of Atapuerca, Spain: possible ancestor to Neandertals and modern humans. Science 276, 1392–1395.

Bermúdez de Castro, J.M., Rosas, A., Nicolás, M.A., 1999a. Dental remains from Atapuerca-TD6 (Gran Dolina site, Burgos, Spain). Journal of Human Evolution 37, 523–566.

Bermúdez de Castro, J.M., Carbonell, E., Cáceres, I., Díez, J.C., Fernández-Jalvo, Y., Mosquera, M., Ollé, A., Rodríguez, J., Rodríguez, X.P., Rosas, A., Rosell, J., Sala, R., Vergés, J.M., van der Made, J., 1999b. The TD6 (Aurora Stratum) hominid site. Final remarks and new questions. Journal of Human Evolution 37, 695–700.

Bermúdez de Castro, J.M., Carretero, J.M., García-González, R., Rodríguez-Gracía, L., Martinón-Torres, M., Rosell, J., Blasco, R., Martín-Francés, L., Modesto, M., Carbonell, E., 2012. Early Pleistocene human humeri from the Gran Dolina-TD6 site (Sierra de Atapuerca, Spain). American Journal of Physical Anthropology 147, 604–617.

Bermúdez de Castro, J.M., Martinón-Torres, M., Sarmiento, S., Lozano, M., 2003. Gran Dolina-TD6 versus Sima de los Huesos dental samples from Atapuerca: Evidence of discontinuity in the European Pleistocene population? Journal of Archaeological Research 30, 1421–1428.

Bermúdez de Castro, J.M., Pérez-González, A., Martinón-Torres, M., Gómez-Robles, A., Rosell, J., Prado, L., Sarmiento, S., Carbonell, E., 2008. A new Early Pleistocene hominin mandible from Atapuerca-TD6, Spain. Journal of Human Evolution 55, 729–735.

Bermúdez de Castro, J.M., Martinón-Torres, M., Gómez-Robles, A., Prado, L., Rosell, J., Gómez-Polín, L., Arsuaga, J.L., Carbonell, E., 2010. New immature hominin fossil from European Lower Pleistocene shows the earliest evidence of a modern human dental development pattern. Proceedings of the National Academy of Sciences USA 107, 11739–11744.

Bermúdez de Castro, J.M., Martinón-Torres, M., Blasco, R., Rosell, J., Carbonell, E., 2013. Continuity or discontinuity in the European Early Pleistocene human settlement: the Atapuerca evidence. Quaternary Science Reviews 76, 53–65.

Bermúdez de Castro, J.M., Quam, T., Martinón-Torres, M., Martínez, I., Gracia-Téllez, A., Arsuaga, J.L., Carbonell, E., 2014. The medial pterygoid tubercle in the Atapuerca Early and Middle Pleistocene mandibles. Evolutionary implications. American Journal of Physical Anthropology 156, 102–109.

Bermúdez de Castro, J.M., Martinón-Torres, M., Rosell, J., Blasco, R., Arsuaga, J.L., Carbonell, E., 2016. Continuity *versus* discontinuity of the human settlement of Europe between the late Early Pleistocene and the early Middle Pleistocene. The mandibular evidence. Quaternary Science Reviews 153, 51–62.

Bermúdez de Castro, J.M., Martinón-Torres, M., Arsuaga, J.L., Carbonell, E., 2017a. Twentieth anniversary of *Homo antecessor* (1997-2017): a review. Evolutionary Anthropology 26, 157–171.

Bermúdez de Castro, J.M., Martinón-Torres, M., Martín-Francés, L., Martínez de Pinillos, M., Modesto-Mata, M., García-Campos, C., Xiujie, W., Xing, S., Wu, L., 2017b. Early Pleistocene hominin deciduous teeth from the *Homo antecessor* Gran Dolina-TD6 bearing level (Sierra de Atapuerca, Spain). American Journal of Physical Anthropology 163, 602–615.

Bermúdez de Castro, J.M., Martinón-Torres, M., Martín-Francés, L., Modesto, M., Martínez de Pinillos, M., García-Campos, C., Carbonell, E., 2017c. *Homo antecessor*. The state of the art eighteen years later. Quaternary International 433, 22–31.

Bermúdez de Castro, J.M., Martinón-Torres, M., Martínez de Pinillos, M., García-Campos, C., Modesto-Mata, M., Martín Francés, L., Arsuaga, J.L., 2018. Metric and morphological comparison between the Arago (France) and Atapuerca-Sima de los Huesos (Spain) dental samples, and the origin of Neanderthals. Quaternary Science Reviews. https://doi.org/10.1016/j.quascirev.2018.04.003.

Boughner, J.C., Hallgrímsson, B., 2008. Biological spacetime and the temporal integration of fuctional modules: a case study of dento-gnathic development timing. Developmental Dynamics 237, 1–17.

Blumberg, J.E., Hylander, W.L., Goepp, R.A., 1971. Taurodontism: A biometric study. American Journal of Physical Anthropology 34, 243–255.

Blumenberg, B., Lloyd, A., 1983. *Australopithecus* and the origin of the genus *Homo*: Aspects of biometry and systematics with accompanying catalog of tooth metric data. ByoSystems 16, 127–167.

Brown, B., Walker, A., 1993. The dentition. In: Walker, A., Leakey, R. (Eds.), The Nariokotome *Homo erectus* Skeleton. Springer-Verlag, Berlin, pp. 161–192.

Butler, M.A., 1995. Ontogenetic aspects of dental evolution. International Journal of Developmental Biology 39, 25–34.

Campaña, I., Pérez-González, A., Benito-Calvo, A., Rosell, J., Blasco, R., Bermúdez de Castro, J.M., Carbonell, E., Arsuaga, J.L., 2016. New interpretation of the Gran Dolina-TD6 bearing *Homo antecessor* deposits through sedimentological analysis. Scientific Reports 6, 34799.

Carbonell, E., Bermúdez de Castro, J.M., Arsuaga, J.L., Díez, J.C., Rosas, A., Cuenca-Bescós, G., Sala, R., Mosquera, M., Rodriguez, X.P., 1995. Lower Pleistocene hominids and artifacts from Atapuerca-TD6 (Spain). Science 269, 826–830.

Carbonell, E., García-Antón, D., Mallol, C., Mosquera, M., Ollé, A., Rodríguez, X.P., Sahnouni, M., Sala, R., Verges, J.M., 1999. The TD6 level lithic industry from Gran Dolina, Atapuerca (Burgos, Spain): production and use. Journal of Human Evolution 37, 653–693.

Carbonell, E., Bermúdez de Castro, J.M., Arsuaga, J.L., Allue, E., Bastir, M., Benito, A., Cáceres, I., Canals, T., Díez, J.C., van der Made, J., Mosquera, M., Ollé, A., Pérez-González, A., Rodríguez, J., Ródríguez, X.P., Rosas, A., Rosell, J., Sala, R., Vallverdú, J., Vergés, J.M., 2005. An early Pleistocene hominin mandible from Atapuerca-TD6, Spain. Proceedings of the National Academy of Sciences USA 102, 5674–5678.

Carbonell, E., Mosquera, M., Rodríguez, X.P., Bermúdez de Castro, J.M., Burjachs, F., Rosell, J., Sala, R., Vallverdú, J., 2008. Eurasian gates: the earliest human dispersals. Journal of Anthropological Research 64, 195–228.

Carlsen, O., 1987. Dental Morphology. Munksgaard, Copenhagen.

Carretero, J.M., Lorenzo, C., Arsuaga, J.L., 1999. Axial and appendicular skeleton of *Homo antecessor*. Journal of Human Evolution 37, 459–499.

Chang, C.-H., Kaifu, Y., Takai, M., Kono, R.T., Grün, R., Matsuura, S., Kinsley, L., Lin, L.-K., 2014. The first archaic *Homo* from Taiwan. Nature Communications 6, 6037.

Crummett, T., 1995. The three dimensions of shovel-shaping. In: Moggi-Cecchi, J. (Ed.), Aspects of Dental Biology: Palaeontology, Anthropology and Evolution. International Institute for the Study of Man, Florence, pp. 305–313.

Cuenca-Bescós, G., Laplana, C., Canudo, J.I., 1999. Biochronological implications of the Arvicolidae (Rodentia, Mammalia) from the Lower Pleistocene hominid-bearing level of Trinchera Dolina 6 (TD6, Atapuerca, Spain). Journal of Human Evolution 37, 353–373.

Cuenca-Bescós, G., Blain, H.-A., Rofes, J., Lozano-Fernández, I., López-García, J.M., Duval, M., Galán, J., Núñez-Lahuerta, C., 2015. Comparing two different Early

Pleistocene microfaunal sequences from the caves of Atapuerca, Sima del Elefante and Gran Dolina (Spain): Biochronological implications and significance of the Jaramillo subchron. Quaternary International 389, 148–158.
Dahlberg, A., 1950. Analysis of the American Indian dentition. In: Brothwell, D.R. (Ed.), Dental Anthropology. Pergamon, Oxford, pp. 149–177.
Daura, J., Sanz, M., Arsuaga, J.L., Hoffman, D.L., Quam, R.M., Ortega, M.C., Santos, E., Gomez, S., Rubio, A., Villaescusa, L., Souto, P., Mauricio, J., Rodrigues, F., Ferreira, A., Godinho, P., Trinkaus, E., Zilhão, J., 2017. New Middle Pleistocene hominin cranium from Gruta da Aroeira (Portugal). Proceedings of the National Academy of Sciences USA 114, 3397–3402.
Demirjian, A., Goldstein, H., Tanner, J.M., 1973. A new system of dental age assessment. Human Biology 45, 211–227.
Dennell, R., Martinón-Torres, M., Bermúdez de Castro, J.M., 2011. Hominid variability, climatic instability and population demography in Middle Pleistocene Europe. Quaternary Science Reviews 30, 1511–1524.
Duval, M., Grün, R., Parés, J.M., Martín-Francés, L., Campaña, I., Rosell, J., Shao, Q., Arsuaga, J.L., Carbonell, E., Bermúdez de Castro, J.M., 2018. The first direct ESR analysis of a hominin tooth from Atapuerca Gran Dolina TD-6 (Spain) supports the antiquity of *Homo antecessor*. Quaternary Geochorology 47, 120–137.
Endicott, P., Ho, S.Y.W., Stringer, C.B., 2010. Using genetic evidence to evaluate four palaeoanthropological hypotheses for the timing of Neanderthal and modern human origins. Journal of Human Evolution 59, 87–95.
Falguères, C., Bahain, J.-J., Yokoyama, Y., Arsuaga, J.L., Bermúdez de Castro, J.M., Carbonell, E., Bischoff, J.L., Dolo, J.-M., 1999. Earliest humans in Europe: the age of Atapuerca fossils, Spain. Journal of Human Evolution 37, 343–352.
Gil, E., Hoyos, M., 1987. Contexto estratigráfico. In: Aguirre, E., Carbonell, E., Bermúdez de Castro, J.M. (Eds.), El Hombre Fósil de Ibeas y el Pleistoceno de la Sierra de Atapuerca. Junta de Castilla y León, Valladolid, pp. 47–55.
Gabounia, L., de Lumley, M.-A., Vekua, A., Lordkipanidze, D., de Lumley, H., 2002. Découverte dun nouvel hominidé à Dmanisi (Transcaucasie, Géogie). Comptes Rendus Palevol 1, 243–253.
Gabunia, L., Vekua, A., 1995. A Plio-Pleistocene hominid from Dmanisi, East Georgia, Caucasus. Nature 373, 509–512.
García, N., Arsuaga, J.L., 1999. Carnivores from the Early Pleistocene hominid-bearing Trinchera Dolina 6 (Sierra de Atapuerca, Spain). Journal of Human Evolution 37, 415–430.
Genet-Varcin, E., 1962. Evolution de la couronne de la seconde prémolaire inférieure chez les hominidés. Annales de Paléontologie 48, 59–81.
Gómez-Robles, A., 2010. Análisis de la forma dental en la filogenia humana. Tendencias y modelos evolutivos basados en métodos de morfometría geométrica. Ph.D. Dissertation, University of Granada.
Gómez-Robles, A., Polly, P.D., 2011. Morphological integrations in the hominin dentition: evolutionary, developmental, and functional factors. Evolution 66, 1024–1033.
Gómez-Robles, A., Martinón-Torres, M., Bermúdez de Castro, J.M., Margvelashvili, A., Bastir, M., Arsuaga, J.L., Pérez-Pérez, A., Estebaranz, F., Martínez, L.M., 2007. A geometric morphometric analysis of hominin upper first molar shape. Journal of Human Evolution 53, 272–285.
Gómez-Robles, A., Martinón-Torres, M., Bermúdez de Castro, J.M., Prado, L., Sarmiento, S., Arsuaga, J.L., 2008. Geometric morphometric analysis of the crown morphology of the lower first premolar of hominins, with special attention to Pleistocene *Homo*. Journal of Human Evolution 55, 627–638.
Gómez-Robles, A., Martinón-Torres, M., Bermúdez de Castro, J.M., Prado-Simón, L., Arsuaga, J.L., 2011a. A geometric morphometric analysis of hominin upper premolars. Shape variation and morphological integration. Journal of Human Evolution 61, 688–702.
Gómez-Robles, A., Bermúdez de Castro, J.M., Martinón-Torres, M., Prado-Simón, L., 2011b. Crown size and cusp proportions in *Homo antecessor* upper first molars. A comment on Quam et al., 2009. Journal of Anatomy 218, 258–262.
Gómez-Robles, A., Bermúdez de Castro, J.M., Martinón-Torres, M., Prado-Simón, L., Arsuaga, J.L., 2015. A geometric morphometric analysis of hominin lower molars: Evolutionary implications and overview of postcanine dental variation. Journal of Human Evolution 82, 34–50.
Green, R.E., Krause, J., Briggs, A.W., Maricic, T., Stenzel, U., Kircher, M., Patterson, N., Li, H., Zhai, W., Fritz, M.H.-Y., Hansen, N.F., Durand, E.Y., Malaspinas, A.-S., Jensen, J.D., Marques-Bonet, T., Alkan, C., Prüfer, K., Meyer, M., Burbano, H.A., Good, J.M., Schultz, R., Aximu-Petri, A., Butthof, A., Höber, B., Höffner, B., Siegemund, M., Weihmann, A., Nusbaum, C., Lander, E.S., Russ, C., Novod, N., Affourtit, J., Egholm, M., Verna, C., Rudan, P., Brajkovic, D., Kucan, Z., Gusic, I., Doronichev, V.B., Golovanova, L.V., Lalueza-Fox, C., de la Rasilla, M., Fortea, J., Rosas, A., Schmitz, R.W., Johnson, P.L.F., Eichler, E.E., Falush, D., Birney, E., Mullikin, J.C., Slatkin, M., Nielsen, R., Kelso, J., Lachmann, M., Reich, D., Pääbo, S., 2010. A draft sequence of the Neandertal genome. Science 328, 710–722.
Grine, F.E., Franzen, J.L., 1994. Fossil hominid teeth from the Sangiran Dome (Java, Indonesia). Courier Forschungsinstitut Senckenberg 171, 75–103.
Hanihara, K., Kuwashima, T., Sakao, N., 1964. The deflecting wrinkle on the lower molars in recent man. Journal of the Anthropological Society of Nippon 72, 1–8.
Hershkovitz, I., Weber, G.W., Quam, R., Duval, M., Grün, R., Kinsley, L., Ayalon, A., Bar-Matthews, M., Valladas, H., Mercier, N., Arsuaga, J.L., Martinón-Torres, M., Bermúdez de Castro, J.M., Fornai, C., Martín-Francés, L., Smith, P., Sarig, R., May, H., Krenn, V.A., Slon, V., Rodríguez, L., García, R., Lorenzo, C., Carretero, J.M., Frumkin, A., Shahack-Gross, R., Bar-Yosef Mayer, D., Cui, Y., Wu, Z., Peled, N., Groman-Yaroslavski, I., Weissbrod, L., Yeshurin, R., Tsatkin, A., Zainder, Y., Weinstein-Evron, M., 2018. The earliest modern humans outside Africa. Science 359, 456–459.
Hlusko, L.J., Mahaney, M., 2009. Quantitative genetics, pleitropy, and morphological integration in the dentition of *Papio hamadryas*. Evolutionary Biology 36, 5–18.
Hlusko, L.J., Sage, R.D., Mahaney, M.C., 2011. Modularity in the mammalian dentition: mice and monkeys share a common dental genetic architecture. Journal of Experimental Zoology 316B, 21–49.
Ho, S.Y.W., Phillips, M.J., Cooper, A., Drummond, A.J., 2005. Time dependency of molecular rate estimates and systematic overestimation of recent divergence times. Molecular Biology and Evolution 22, 1561–1568.
Hrdlicka, A., 1924. New data on the teeth of early man and certain fossil European apes. American Journal of Physical Anthropology 7, 109–132.
Hublin, J.-J., Ben-Ncer, A., Bailey, S.E., Freidline, S.E., Neubauer, S., Skinner, M.M., Bergmann, I., Le Cabec, A., Benazzi, S., Harvati, K., Gunz, P., 2017. New fossils from Jebel Irhoud, Morocco and the pan-African origin of *Homo sapiens*. Nature 546, 289–292.
Irish, J.D., 1993. Biological affinities of late Pleistocene through modern African Aboriginal populations: the dental evidence. Ph.D. Dissertation, Arizona State University.
Johanson, D.C., White, T.D., Coppens, Y., 1978. A new species of the genus *Australopithecus* (Primates: Hominidae) from the Pliocene of eastern Africa. Kirtlandia 28, 1–14.
Kaifu, Y., Baba, H., Aziz, F., Indriati, E., Schrenk, F., Jacob, T., 2005a. Taxonomic affinities and evolutionary history of the early Pleistocene hominids of Java: dentognathic evidence. American Journal of Physical Anthropology 128, 709–726.
Kaifu, Y., Aziz, F., Baba, H., 2005b. Hominid mandibular remains from Sangiran: 1952–1986 collection. American Journal of Physical Anthropology 128, 497–519.
Kaifu, Y., Kono, R.T., Sutikna, T., Saptomo, E.W., 2015. Unique dental morphology of *Homo floresiensis* and its evolutionary implications. PLoS One 10, e0141614.
Kieser, J.A., 1990. Human Adult Odontometrics. Cambridge University Press, Cambridge.
Kieser, J.A., Groeneveld, H.T., 1987. Tooth size and arcadal length correlates in man. International Journal of Anthropology 2, 37–46.
Kimbel, W.H., Johanson, D.C., Rak, Y., 1997. Systematic assessment of a maxilla of *Homo* from Hadar, Ethiopia. American Journal of Physical Anthropology 103, 235–262.
Klingenberg, C.P., 2008. Morphological integration and development modularity. Annual Review of Ecology, Evolution and Systematics 39, 115–132.
Krause, J., Fu, Q., Good, J.M., Viola, B., Shunkov, M.V., Derevianko, A.P., Pääbo, S., 2010. The complete mitocondrial DNA genome of an unknown hominin from southern Siberia. Nature 464, 894–897.
Kricun, M., Monge, J., Mann, A., Finkel, G., Lampl, M., Radovcic, J., 1999. The Krapina Hominids: a Radiographic Atlas of the Skeletal Collection. Croatian Natural History Museum, Zagreb.
Kupczik, K., Hublin, J.-J., 2010. Mandibular molar roots morphology in Neanderthals and Late Pleistocene and recent *Homo sapiens*. Journal of Human Evolution 59, 525–541.
Langergraber, K.E., Prüfer, K., Rowney, C., Boesch, C., Crockford, C., Fawcett, K., Inoue, E., Inoue-Muruyama, M., Mitano, J.C., Muller, M.N., Robbins, M.M., Schubert, G., Stoinski, T.S., Viola, B., Watts, D., Wittig, R.M., Wrangham, R.W., Zuberbühler, K., Pääbo, S., Vigilant, L., 2012. Generation times in wild chimpanzees and gorillas suggest earlier divergence times in great ape and human evolution. Proceedings of the National Academy of Sciences USA 109, 15716–15721.
Lefèvre, J., 1973. Etude odontologique des hommes de Muge. Bulletin et Mémoires de la Societé d'Anthropologie de Paris 12, 301–333.
Liu, W., Martinón-Torres, M., Kaifu, Y., Xiujie, W., Kono, R.T., Chang, C.-H., Wei, P., Song, X., Huang, W., Bermúdez de Castro, J.M., 2017. A mandible from the Middle Pleistocene site of Hexian (Eastern China) and its significance on the variability of Asian *Homo erectus*. American Journal of Physical Anthropology 162, 715–731.
Lumley, H.D., Lumley, M.D., Brandi, R., Guerrier, E., Pillard, F., Pillard, B., 1972. La Grotte Moustérienne de Hortus. Editions du Laboratoire de Paléontologie Humaine et de Préhistoire, Marseille.
van der Made, J., 1999. Ungulates from Atapuerca TD6. Journal of Human Evolution 37, 389–413.
Martínez de Pinillos, M., Martinón-Torres, M., Skinner, M.M., Arsuaga, J.L., Gracia-Téllez, A., Martínez, I., Martín-Francés, L., Bermúdez de Castro, J.M., 2014. Trigonid crests expression in Atapuerca-Sima de los Huesos lower molars: internal and external morphological expression and evolutionary inferences. Comptes Rendus Palevol 13, 205–221.
Martínez de Pinillos, M., Martinón-Torres, M., Martín-Francés, L., Arsuaga, J.L., Bermúdez de Castro, J.M., 2017. Comparative analysis of the trigonid crests patterns in *Homo antecessor* molars at the enamel and dentine surfaces. Quaternary International 433, 189–198.
Martinón-Torres, M., 2006. Evolución del aparato dental en homínidos: estudio de los dientes humanos del Pleistoceno de Sierra de Atapuerca, Burgos. Ph.D. Dissertation, University of Santiago de Compostela.
Martinón-Torres, M., Bermúdez de Castro, J.M., Gómez-Robles, A., Arsuaga, J.L., Carbonell, E., Lordkipanidze, D., Manzi, G., Margvelashvili, A., 2007. Dental evidence on the hominin dispersals during the Pleistocene. Proceedings of the National Academy of Sciences USA 104, 13279–13282.
Martinón-Torres, M., Bermúdez de Castro, J.M., Gómez-Robles, A., Margvelashvili, A., Lordkipanidze, D., Vekua, A., 2008. Dental remains from

Dmanisi: Morphological analysis and comparartive study. Journal of Human Evolution 55, 249–273.
Martinón-Torres, M., Bermúdez de Castro, J.M., Gómez-Robles, A., Prado-Simón, L., Arsuaga, J.L., 2012. Morphological description and comparison of the dental remains from Atapuerca-Sima de los Huesos site (Spain). Journal of Human Evolution 62, 7–58.
Martinón-Torres, M., Spěváčková, P., Gracia-Téllez, A., Martínez, I., Bruner, E., Arsuaga, J.L., Bermúdez de Castro, J.M., 2013. Morphometric analysis of molars in a Middle Pleistocene population shows a mosaic of "modern" and Neanderthal features. Journal of Anatomy 223, 353–363.
Meyer, M., Arsuaga, J.L., de Filippo, C., Nagel, S., Aximu-Petri, A., Nickel, B., Martínez, I., Gracia, A., Bermúdez de Castro, J.M., Carbonell, E., Viola, B., Kelso, J., Prüfer, K., Pääbo, S., 2016. Nuclear DNA sequences from the Middle Pleistocene Sima de los Huesos hominins. Nature 531, 504–507.
Miller, E.H., Sung, H.-C., Moulton, V.D., Miller, G.W., Finley, J.K., Stenson, G.B., 2007. Variation and integration of the simple mandibular postcanine dentition in two species of phicid seal. Journal of Mammalogy 88, 1325–1334.
Mizoguchi, Y., 1981. Variation units in the human permanent dentition. Bulletin of the National Science Museum Tokyo 7, 29–39.
Mizoguchi, Y., 1985. Shovelling: A Statistical Analysis of its Morphology. The University of Tokyo Press, Tokyo.
Moggi-Cecchi, J.M., Grine, F.E., Tobias, P.V., 2006. Early hominid dental remains from Members 4 and 5 of the Sterkfontein Formation (1966–1996 excavations): Catalogue, individual associations, morphological descriptions, and initial metric analysis. Journal of Human Evolution 50, 239–328.
Molnar, S., 1971. Human tooth wear, tooth function and cultural variability. American Journal of Physical Anthropology 34, 175–190.
Moreno, D., Falguères, C., Pérez-González, A., Voinchet, P., Ghaleb, B., Despriee, J., Bahain, J.J., Sala, R., Carbonell, E., Bermúdez de Castro, J.M., Arsuaga, J.L., 2015. New radiometric dates on the lowest stratigraphical section (TD1 to TD6) of Gran Dolina site (Atapuerca, Spain). Quaternary Geochronology 30, 535–540.
Mounier, A., Mirazón Lahar, M., 2016. Virtual ancestor reconstruction: Revealing the ancestor of modern humans and Neandertals. Journal of Human Evolution 91, 57–72.
Ortiz, A., Skinner, M.M., Bailey, S.E., Hublin, J.J., 2012. Carabelli's trait revisited: an examination of mesiolingual features at the enamel-dentine junction and enamel surface of *Pan* and *Homo sapiens* upper molars. Journal of Human Evolution 63, 586–596.
Ovchinnikov, I.V., Gotherstrom, A., Romanova, G.P., Kharitonov, V.M., Liden, K., Goodwin, W., 2000. Molecular analysis of Neanderthal DNA from the northern Caucasus. Nature 404, 490–493.
Parés, J.M., Pérez-González, A., 1995. Paleomagnetic age for hominid fossils at Atapuerca archaeological site, Spain. Science 269, 830–832.
Parés, J.M., Pérez-González, A., 1999. Magnetochronology and stratigraphy at Gran Dolina section, Atapuerca (Burgos, Spain). Journal of Human Evolution 37, 325–342.
Parés, J.M., Sier, M., Duval, M., Woodhead, J., Carbonell, E., Álvarez-Posada, C., Campaña, I., Moreno, D., Ortega, A.I., Bermúdez de Castro, J.M., Rosell, J., 2018. Chronology of the cave interior sediments at Gran Dolina archaeological site, Atapuerca (Spain). Quaternary Science Reviews 186, 1–16.
Patte, É., 1962. La Dentition des Néanderthaliens. (Annales de Paléontologie 45–47), Masson et Cie. Paris.
Plavcan, J.M., Daegling, D.J., 2006. Interspecific and intraspecific relationships between tooth size and jaw size in primates. Journal of Human Evolution 51, 171–184.
Prado-Simón, L., Martinón-Torres, M., Baca, P., Gómez-Robles, A., Bermúdez de Castro, J.M., 2011. A morphological study of the tooth roots of the Sima del Elefante mandible (Atapuerca, Spain): a new classification of the teeth—biological and methodological considerations. Anthropological Sciences 120, 61–72.
Reich, D., Green, R.E., Kircher, M., Krause, J., Patterson, N., Durand, E.Y., Viola, B., Briggs, A.W., Stenzel, U., Johnson, P.L.F., Maricic, T., Good, J.M., Marques-Bonet, T., Alkan, C., Fu, O., Mallick, S., Li, H., Meyert, M., Eichler, E.E., Stoneking, M., Richards, M., Talamo, S., Shunkov, M.V., Derevianko, A.P., Hublin, J.J., Kelso, J., Slakin, M., Pääbo, S., 2010. Genetic history of an archaic group from Denisova cave in Siberia. Nature 468, 1053–1060.
Rightmire, G.P., Lorkipanidze, D., Vekua, A., 2006. Anatomical descriptions, comparative studies and evolutionary significance of the hominin skulls from Dmanisi, Republic of Georgia. Journal of Human Evolution 50, 115–141.
Rightmire, G.P., Ponce de León, M.S., Lordkipanidze, D., Margvelashvili, A., Zollikofer, P.E., 2017. Skull 5 from Dmanisi: Descriptive anatomy, comparative studies, and evolutionary significance. Journal of Human Evolution 104, 50–79.
Robinson, J.T., 1956. The Dentition of the Australopithecinae. Transvaal Museum Memoir No 9, Pretoria.
Roksandic, M., Mihailovic, D., Mercier, N., Dimitrijevic, V., Morley, M.W., Rakocevic, Z., Mihailovic, B., Guibert, P., Babb, J., 2011. A human mandible (BH1) from the Pleistocene deposits of Mala Balanica cave (Sicevo Gorge, Nis, Serbia). Journal of Human Evolution 61, 186–196.
Rosas, A., Bermúdez de Castro, J.M., 1998. On the taxonomic affinities of the Dmanisi mandible (Georgia). American Journal of Physical Anthropology 107, 145–162.
Sakuma, M., Yamamoto, M., Takahiko, O., 1987. On the deflecting wrinkle in the lower molars of Malawians derived from pureblooded Negroid racial stock. Japanese Journal of Oral Biology 29, 371–377.
Scott, G.R., Turner II, C.G., 1997. The Anthropology of Modern Human Teeth: Dental Morphology and its Variation in Recent Human Populations. Cambridge University Press, Cambridge.
Shaw, J.C.M., 1928. Taurodont teeth in South African races. Journal of Anatomy 62, 476–498.
Sperber, G., 1973. Morphology of the check teeth of early South African hominids. Ph.D. Dissertation, University of Witwatersrand.
Stock, D.W., 2001. The genetic basis of modularity in the development and evolution of the vertebrate dentition. Philosophical Transactions of the Royal Society of London B 356, 1633–1653.
Suwa, G., Asfaw, B., Haile-Selassie, Y., White, T., Katoh, S., WoldeGabriel, G., Hart, W.K., Nakaya, H., Beyene, Y., 2007. Early Pleistocene *Homo erectus* fossils from Konso, southern Ethiopia. Anthropological Science 115, 133–151.
Tattersall, I., 2011. Before the Neanderthals: Hominid Evolution in Middle Pleistocene Europe. In: Condemi, S., Weniger, G.-C. (Eds.), Before the Neanderthals: Hominid Evolution in Middle Pleistocene Europe. Springer Science. Business Media B.V., New York, pp. 47–53.
Tobias, P.V., 1991. Olduvai Gorge. In: The Skulls, Endocasts and Teeth of *Homo habilis*, vol. 4. Cambridge University Press, Cambridge.
Toro-Moyano, I., Martínez-Navarro, B., Agustí, J., Souday, C., Bermúdez de Castro, J.M., Martinón-Torres, M., Fajardo, B., Duval, M., Falguères, C., Oms, O., Parés, J.M., Anadón, P., Juliá, R., García-Aguilar, J.M., Moigne, A.-M., Espigares, M.P., Ros-Montoya, S., Palmqvist, P., 2013. The oldest human fossil in Europe from Orce (Spain). Journal of Human Evolution 65, 1–9.
Turner II, C.G., Nichol, C.R., Scott, G.R., 1991. Scoring procedures for key morphological traits of the permanent dentition: The Arizona State University Dental Anthropology System. In: Kelley, M., Larsen, C. (Eds.), Advances in Dental Anthropology. Wiley-Liss, New York, pp. 13–31.
Trinkaus, E., Bailey, S.E., Zilhão, J., 2001. Upper Paleolithic human remains from the Gruta do Caldeirão, Tomar, Portugal. Revista Portuguesa de Arqueologia 4, 5–13.
Ward, S.C., Johanson, D.C., Coppens, Y., 1982. Subocclusal morphology and alveolar process relationships of hominid gnathic elements from the Hadar Formation: 1974–1977 collections. American Journal of Physical Anthropology 57, 605–630.
Weidenreich, F., 1937. The dentition of *Sinanthropus pekinensis*: A comparative odontography of the hominids. Palaeontologica Sinica 1, 1–180.
Wolpoff, M.H., 1971. Metric Trends in Hominid Dental Evolution. Case Western Reserve University Press, Cleveland.
Wolpoff, M.-H., 1980. Paleoanthropology. Alfred A. Knopf, New York.
Wood, B., 1991. Hominid Cranial Remains. Koobi Fora Research Project, vol. 4. Clarendon Press, Oxford.
Wood, B.A., Engleman, C.A., 1988. Analysis of the dental morphology of Plio-Pleistocene hominids: V. Maxillary postcanine tooth morphology. Journal of Anatomy 161, 1–35.
Wood, B.A., Uytterschaut, H., 1987. Analysis of the dental morphology of Plio-Pleistocene hominins. III. Mandibular premolar crowns. Journal of Anatomy 154, 121–156.
Wood, B.A., Abbott, S.A., Uytterschaut, H., 1988. Analysis of the dental morphology of Plio-Pleistocene hominids. Journal of Anatomy 156, 107–139.
Xing, S., Martinón-Torres, M., Bermúdez de Castro, J.M., Zhang, Y., Fan, X., Zheng, L., Huang, W., Wu, L., 2014. Middle Pleistocene hominin teeth from Longtan Cave, Hexian, China. PLoS One 9, e114265.
Xing, S., Martinón-Torres, M., Bermúdez de Castro, J.M., 2018. The fossil teeth of Peking Man. Scientific Reports 8, 2066.
Xing, S., Sun, C., Martinón-Torres, M., Bermúdez de Castro, J.M., Han, F., Zhang, Y., Liu, W., 2016. Hominin teeth from the Middle Pleistocene site of Yiyuan, Eastern China. Journal of Human Evolution 95, 33–54.
Zanolli, C., 2013. Additional evidence for morpho-dimensional tooth crown variation in a new Indonesian *H. erectus* sample from the Sangiran Dome (Central Java). PLoS One 8, e67233.
Zanolli, C., Mazurier, A., 2013. Endostructural characterization of the *H. heidelbergensis* dental remains from the early Middle Pleistocene site of Tighenif, Algeria. Comptes Rendus Palevol 12, 293–3014.
Zanolli, C., Bondioli, L., Coppa, A., Dean, C.M., Bayle, P., Candilio, F., Capuani, S., Dreossi, D., Fiore, I., Frayer, D.W., Libsekai, Y., Mincini, L., Rook, L., Medin Tekle, T., Tuniz, C., Macchiarelli, R., 2014. The late Early Pleistocene human dental remains from Uadi Aalad and Mulhuli-Amo (Buia), Eritrean Danakil: Macromorphology and microstructure. Journal of Human Evolution 74, 96–113.
Zanolli, C., Pan, L., Dumoncel, J., Kullmer, O., Kundrat, M., Wu, L., Macchiarelli, R., Mancini, L., Schrenck, F., Tuniz, C., 2018. Inner tooth morphology of *Homo erectus* from Zhoukoudian. New evidence from an old collection housed at Uppsala University, Sweden. Journal of Human Evolution 116, 1–13.
Zilhão, J., 1997. O paleolítico Superior da Estremadura Portuguesa. Colibri, Lisboa.
Zubov, A.A., 1992. The epicristid or middle trigonid crest defined. Dental Anthropology Newsletter 6, 9–10.